Myhre, A.M., Thiede, J., Firth, J.V., et al., 1995
Proceedings of the Ocean Drilling Program, Initial Reports, Vol. 151

13. CENOZOIC NORTHERN HEMISPHERE POLAR AND SUBPOLAR OCEAN PALEOENVIRONMENTS (SUMMARY OF ODP LEG 151 DRILLING RESULTS)[1]

Jörn Thiede,[2] A.M. Myhre,[3] J.V. Firth,[4] and the Shipboard Scientific Party[5]

ABSTRACT

Leg 151 of the Ocean Drilling Program (July to September 1993, St. John's, Newfoundland, to Reykjavik, Iceland) visited the northernmost North Atlantic (Iceland Sea, Greenland Sea, Fram Strait) and Arctic Ocean (northern Fram Strait, Yermak Plateau) to sample basement rocks and overlying sedimentary sequences. The aims were to determine the nature of the basement in several of the drilled areas, and to establish the paleoenvironmental, paleoceanographic, and paleoclimatic record of the Cenozoic Northern Hemisphere. Leg 151 was the first leg to study the problems, impact, and history of North Atlantic-Arctic Gateways. It was also the first attempt ever to drill marginal areas of the Arctic Ocean proper.

The major scientific accomplishments of Leg 151 drilling are:

1. Recovery of a unique Oligocene deep neritic to bathyal sequence on the Hovgaard Ridge (Fram Strait, Site 908);
2. Recovery of a thick sequence of Quaternary to Miocene (Oligocene?) sediments in the center of Fram Strait, close to the modern sill between the Arctic Ocean and the Norwegian-Greenland Sea (Site 909);
3. Discovery of extraordinarily thick Pliocene and Quaternary Arctic Ocean sediments found on Yermak Plateau (Sites 910, 911, 912);
4. Discovery of overconsolidated sediments that document the extension of the Quaternary Barents Sea ice sheets more than 100 km North of Svalbard (Site 910);
5. Recovery of a thick Quaternary glacial sediment sequence with numerous ice-rafted dropstones, and of middle Miocene and Paleogene pelagic sediments on the East Greenland Margin (Site 913);
6. Determination of Milankovitch-type frequency variations in many bulk sediment properties at the Iceland Plateau (Site 907).

HISTORY AND DYNAMICS OF NORTH ATLANTIC–ARCTIC GATEWAYS

The Cenozoic opening of the northern North Atlantic and the breakthrough of deep-water passages between the Arctic Ocean in the North and the main North Atlantic basin in the South had profound consequences for world ocean circulation and for Northern Hemisphere climates. The gateways between the Arctic Ocean and the North Atlantic (Fram Strait and the overflow across the Greenland-Scotland Ridge) are two of the most important and sensitive passages for surface and bottom waters of the world ocean. Leg 151 was designed to describe and decipher the geological history of these gateways and to relate changes in the patterns of sedimentation to the plate tectonic and paleoclimatic history of the Northern Hemisphere.

The early Tertiary lithospheric breakup between Eurasia and Greenland occurred at the time of magnetic Chron C24.r, close to the Paleocene/Eocene boundary. The late syn-rift phase led to extensive uplift and formation of a land area along the subsequent breakup axis. Extensive transient igneous activity accompanied the breakup and both intrusive and extrusive complexes were emplaced along the continental margins, including onshore flood basalts. A more persistent part of the volcanic activity is the Greenland-Scotland Ridge. The subsequent plate tectonic evolution of the Norwegian-Greenland Sea can be divided into two major phases: (1) Between breakup and Chron C13 (Eocene/Oligocene boundary), Greenland was moving in a Northwest direction with respect to Eurasia, with spreading in the Norwegian and the southernmost part of the Greenland seas while transtensional and transpressional movements took place along the transform between Greenland and Svalbard; (2) Chron C13 time was marked by a change in the pole of rotation; the northern Greenland Sea began to open and the Hovgaard Ridge microcontinent was cut off from the Svalbard Margin. The efficacy of the Fram Strait as a deep water passage was delayed by the subsidence of the subaerially created Yermak Plateau and Morris Jesup Rise. These volcanic features probably have a hot-spot origin dating from Chron C18 to C13 time.

Several Deep Sea Drilling Project (DSDP) and Ocean Drilling Program (ODP) expeditions to the northern polar and subpolar deep-sea regions have allowed us to slowly unravel the evolution and origin of one of the most important events in Earth's history: the cooling and eventual glaciation of the polar and subpolar regions. In this chapter, we outline in various ways the state-of-the-art knowledge of the paleoceanographic history of the Norwegian-Greenland Sea and the gateways between the Arctic and North Atlantic oceans. Figure 1A shows the main bathymetric and plate tectonic features of the areas under study, with locations of sites drilled during Leg 151.

NARRATIVE OF LEG 151

An eventful and exciting episode of Arctic exploration began when *JOIDES Resolution* sailed out of the harbor at St. John's, New-

[1]Myhre, A.M., Thiede, J., Firth, J.V., et al., 1995. *Proc. ODP, Init. Repts.*, 151: College Station, TX (Ocean Drilling Program).

[2]GEOMAR Research Center for Marine Geosciences, Wischhofstrasse 1-3, D-24148 Kiel, Federal Republic of Germany.

[3]Department of Geology, University of Oslo, N-0316 Oslo, Norway.

[4]Ocean Drilling Program, Texas A&M University Research Park, 1000 Discovery Drive, College Station, TX 77845, U.S.A.

[5]Shipboard Scientific Party is as given in the list of participants preceding the Table of Contents.

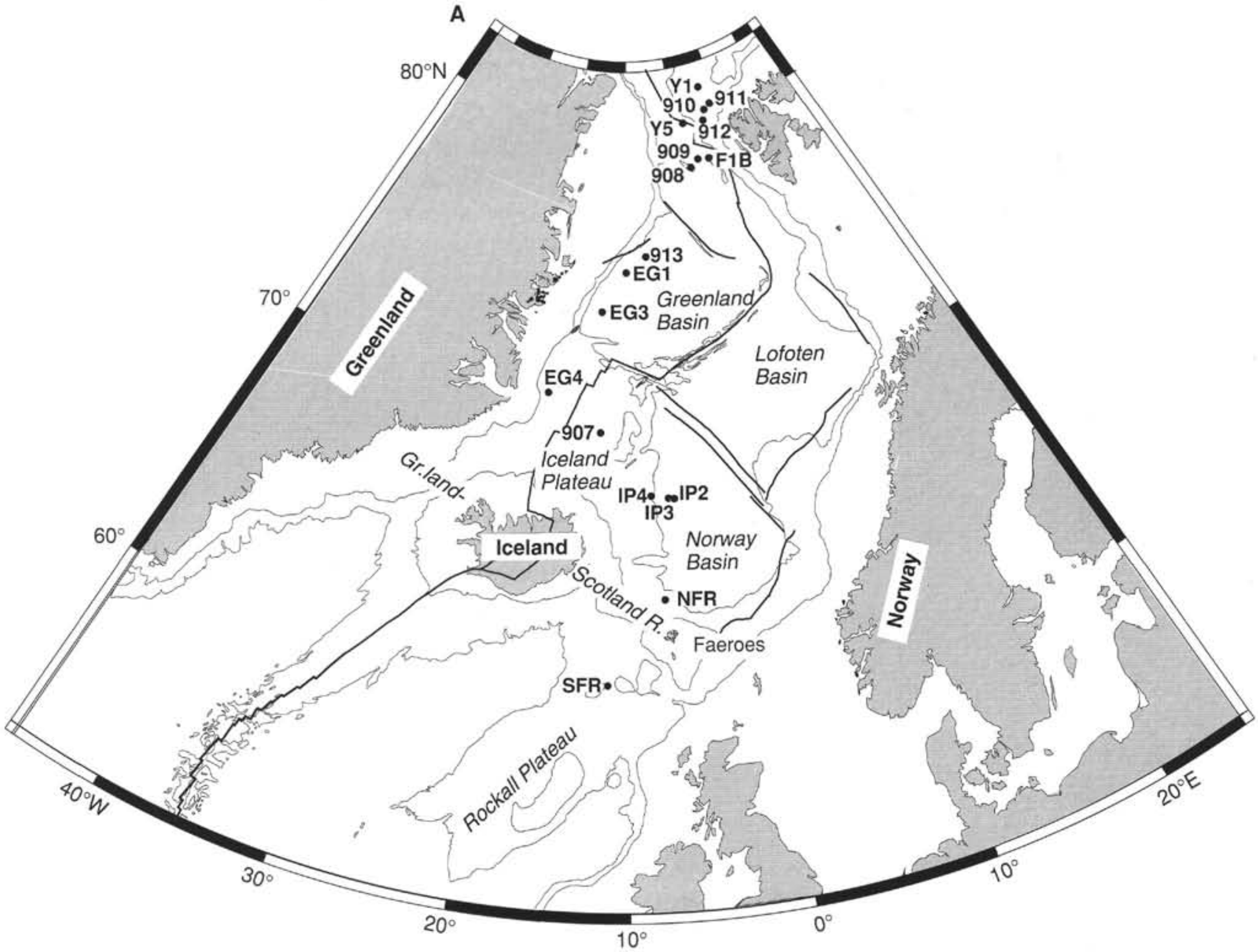

Figure 1. **A.** Simplified bathymetric map of the Norwegian-Greenland Sea, showing location of drilled and proposed sites for Leg 151. **B.** Oceanography and ice cover of the modern Norwegian-Greenland Sea and Fram Strait (from Gascard et al., 1988).

foundland, Canada, on July 29, 1993. ODP Leg 151 was dedicated to bringing the drill ship to the highest northern latitudes (Fig. 1) ever attempted, in order to collect data on past environmental variability that are crucial for progress in climate forecasting on mid- to long-term time scales. The operators of the ship as well as the scientific community were willing to enter the ice-infested Arctic waters after a careful survey of the available data on ice distributions and movements (Wadhams, 1991) in the northern Norwegian-Greenland Sea, Fram Strait, and the adjacent marginal region of the Arctic Ocean had indicated a high probability of reaching most of the selected site locations. In addition, ODP contracted extensive ice-forecasting services from the Nansen Environmental Remote Sensing Center (NERSC) in Bergen, Norway. German, Canadian, and Norwegian official weather services also provided special ice reports. For operations in the immediate neighborhood of the ice margin, the Finnish icebreaker *Fennica* was chartered for ice patrol and safety services. *Fennica* and *JOIDES Resolution* rendezvoused in Fram Strait in mid-August.

Operations began at one of the southern sites on the central eastern Iceland Plateau to exploit the optimal weather window at the northernmost sites during late August–early September. After the sea voyage around the southern tip of Greenland and through the Denmark Strait and after a brief seismic survey, *JOIDES Resolution* reached Site 907 on the morning of 5 August 1993. The site had been chosen to obtain a high-resolution, carbonate-rich pelagic Neogene and Quaternary sedimentary section that was to be triple-cored to acquire a stratigraphically complete section. Hole 907A, in 1800.8 m of water, was APC/XCB cored to volcanic basement at 216.3 mbsf and penetrated another 7.8 m into basement. After four logging runs were completed, operations at this site ended prematurely because one of the crew members fell ill and required immediate medical evacuation. At the advice of the Icelandic coast guard, the U.S. Air Force Base at Keflavik was contacted, and two Blackhawk helicopters and a C-130 Hercules fixed-wing plane were sent to a rendezvous point Northwest of Iceland where the evacuation was completed in the early afternoon of 7 August 1993.

Rather than return to Site 907, we decided to bypass it and proceed directly to the Fram Strait in anticipation of meeting *Fennica*. Site 908 (Hovgaard Ridge) was reached on 12 August 1993, after a brief site survey. The coring program consisted of two APC/XCB holes in 1273.6 m of water, planned to penetrate through a seismically well-expressed unconformity into an older stratified sediment sequence. Heat-flow measurements established a temperature gradient of 54.8°C/km. After reaching a depth of 344.6 mbsf, drilling was terminated when the XCB cutting shoe packed off with clay, overheated by friction, and broke circumferentially in the threads. Despite difficult hole conditions, three successful logging runs were completed. Hole 908B penetrated the upper part of the sedimentary column to 83.4 mbsf.

We then proceeded to Site 909 while awaiting the arrival of *Fennica* and the determination of ice conditions on the Yermak Plateau.

B

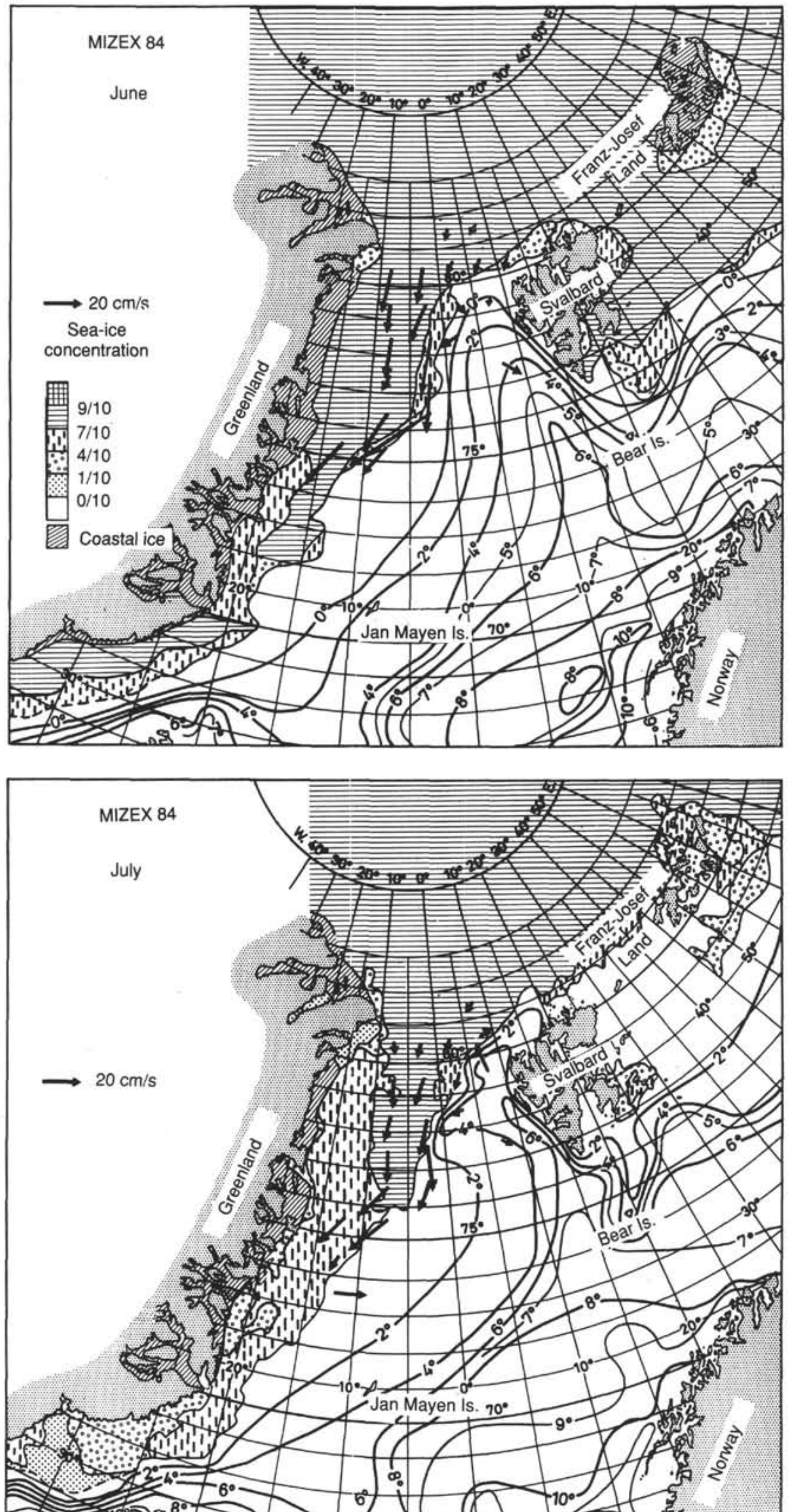

Figure 1 (continued).

Site 909 is located on a deep terrace in 2519 m of water about 18 nmi Northeast of Site 908, on a sill between the Arctic Ocean and the Norwegian-Greenland Sea, which has apparently undisturbed pelagic sedimentation.

Fennica arrived at Site 909 on 16 August 1993, and personnel were transferred for mutual consultations. *Fennica* brought two scientists from the Scott Polar Research Institute (Cambridge University, U.K.) who performed ice observations. A German TV crew from NDR (Norddeutscher Rundfunk) had also accompanied the icebreaker from Stavanger, Norway, in preparation for a comprehensive TV news report on Leg 151. The TV crew later visited the drill ship for extended periods to document the complex deep-sea drilling operations in ice-infested waters. Later on 16 August, *Fennica* departed *JOIDES Resolution* to determine the nature and location of the pack-ice margins at the proposed drill sites nearest the drill ship. The ice edge was found to be composed of a mixture of slush and rotten first-year ice, 1–1.5 m thick and in 20 × 20 m blocks. The marginal ice zone was scattered, but loose ice was not found in the immediate area or near planned Site YERM-4. Later during the cruise *Fennica* was frequently sent out on scouting trips because the satellite imagery received via NERSC was not detailed enough for day-to-day site operations close to the ice margins. Cooperation with the icebreaker was uncomplicated and efficient.

After Holes 909A and 909B were cored to APC-refusal, *Fennica* reported that some of the YERM sites were ice-free. We proceeded North to begin flexible operations at sites very close to the ice margin. These efforts, however, were frustrated by the rapid, unpredictable movements of the ice margin. The drill ship arrived on 17 August at Site 910, in 556.4 m of water approximately 100 km North-Northwest of Svalbard. Drilling encountered unexpected problems because of overconsolidated sediments that were sampled later in the cruise in a special hole (910D) specifically dedicated to investigations of the geotechnical properties of these deposits. Operations at Site 910 (Holes A–C) continued until 20 August when a broad ice front drifted toward the drill ship. This ice field contained bergy bits up to 3 m thick, and *Fennica* was called back to provide assistance and to patrol the ice situation in the immediate neighborhood of the site.

Site 911 was reached on 22 August on the Yermak Plateau in 901.6 m of water, where APC/XCB coring was conducted. As at the other sites on the Yermak Plateau and in Fram Strait, drilling operations were plagued by high gas content. Monitoring of the gas concentrations established that it was mostly of biogenic origin and did not present an immediate danger to ship or drilling operations, but gas expansion in the core liners caused considerable core disturbance. After completion of Hole 911A, three logging runs were successfully completed, and coring operations resumed in Holes 911B and 911C.

In the meantime, *Fennica* scouted the ice situation at the proposed site locations farther North and West. The northernmost site was ice covered, and therefore we proceeded to Site 912, which, however, was also located rather close to a 15-nmi-long, 0.1-nmi-wide ice tongue. As soon as we began operations at Site 912 on 27 August, the ice tongue began moving, and despite the efforts of *Fennica* the drill ship was forced off location after coring to only 145.4 mbsf in Hole 912A. Hole 912B had to be abandoned at a depth of 40.5 mbsf, despite every effort by the icebreaker to fend off the ice, and the pipe had to be pulled above the seafloor. The drill ship moved away from the site in dynamic positioning (DP) mode in the hope of returning. However, after monitoring the ice for 6 hours, we decided to return to Site 910 to drill a geotechnical hole (910D). Operations to complete this hole were uncomplicated, and these special cores were stored vertically and not opened to avoid any disturbance of their geotechnical properties.

On 29 August, *Fennica* was sent to the proposed northernmost site location to report on the ice conditions. This site was found under a thick and dense cover of old sea ice. Therefore, a new location was proposed situated approximately 10 nmi farther South, in open waters and in an identical setting according to the seismic data. The drill ship proceeded to this location, and the drill string was lowered to just above the seafloor. Despite the approval of the ODP Safety Panel, extensive efforts of ODP personnel in Texas, and against the expectations of the ODP Leg 151 Scientific Party, the Norwegian Petroleum Directorate declined permission to drill this site in the first round of negotiations. Permission was obtained two days later, but by then the drill ship had departed, and on later occasions the site was never again ice-free.

When the Norwegian permission was denied, the drill string was pulled, and preparations were made to return to Site 912 (with Site 909 as the alternate). The Site 912 location was found completely within heavy pack ice, and the drill ship bypassed the site and continued to Site 909 to core a deep RCB hole, in the hope that the ice might relocate in the meantime to free some of the desired locations farther North. We arrived at Site 909 on 31 August. Hole 909C was RCB-cored down to 1061.8 mbsf. Heat-flow measurements taken in Hole 909A established a temperature gradient of 97.6°C/km. A steadily increasing deviation from the vertical ranging from 14° at 600 mbsf to a maximum of 25.6° at 1010 mbsf was observed in Hole 909C. Hole 909C was terminated at 1061.8 mbsf because heavier hydrocarbons began to appear. Their concentrations increased strongly and abruptly, and a light-yellow fluorescence was observed. The deepest cores had a strong petroleum odor. Kerogen slides indicated a large amount of thermally mature kerogen, and total organic carbon increased from 1% to 2.6%. After successful logging of the hole, a 41-m-thick cement plug was set, and the hole was loaded with heavy mud. Hole 909C ended on 11 September.

Meanwhile *Fennica* sailed North again to scout the ice situation. It had to be recalled to *JOIDES Resolution*, however, to deliver the German NDR TV crew for pickup by helicopter. The helicopter arrived on 5 September, bringing ODP personnel and two technical specialists for *Fennica*. The four incoming personnel were transferred immediately to *Fennica*. The icebreaker then returned to ice patrol. Ice conditions to the North and West were not favorable. The drill ship returned to Site 912, but was forced to abandon location after drilling to only 209.1 mbsf. As an icebreaker was not thought to be necessary at the next site, *Fennica* was released on 13 September, 1993.

JOIDES Resolution arrived at Site 913 on 14 September, in 3318.6 m of water off East Greenland. Unexpectedly, the site survey could not be conducted as planned, owing to extensive and rapidly moving ice fields. Hole 913A was APC/XCB cored, but because of the unconsolidated nature of the relatively coarse sediments and the abundant large dropstones, recovery was abysmal. The hole was terminated at 103.6 mbsf because of the slow penetration rate of the XCB system. An RCB BHA was run for Hole 913B. Recovery was very poor again, and it was decided to wash extended intervals with spot coring attempts until recovery improved, which happened close to 420 mbsf. After penetrating about 250 m farther down the section with moderate to good recoveries, unconsolidated silts with some hard carbonate-rich sandstones were encountered, resulting again in very poor recoveries.

Coring was terminated when time ran out on 20 September 1993. *JOIDES Resolution* needed 81 hrs for the transit to Reykjavik, Iceland, where Leg 151 ended on 24 September 1993.

DRILLING RESULTS BY LOCATION: GEOLOGICAL SUMMARIES, SITES 907–913

Site 907

Site 907, located on the eastern Iceland Plateau, was APC/XCB cored to 224.1 mbsf, encountering basalt in the lower 7.8 m. Five sedimentary lithostratigraphic units are recognized (Figs. 2 and 3): Unit

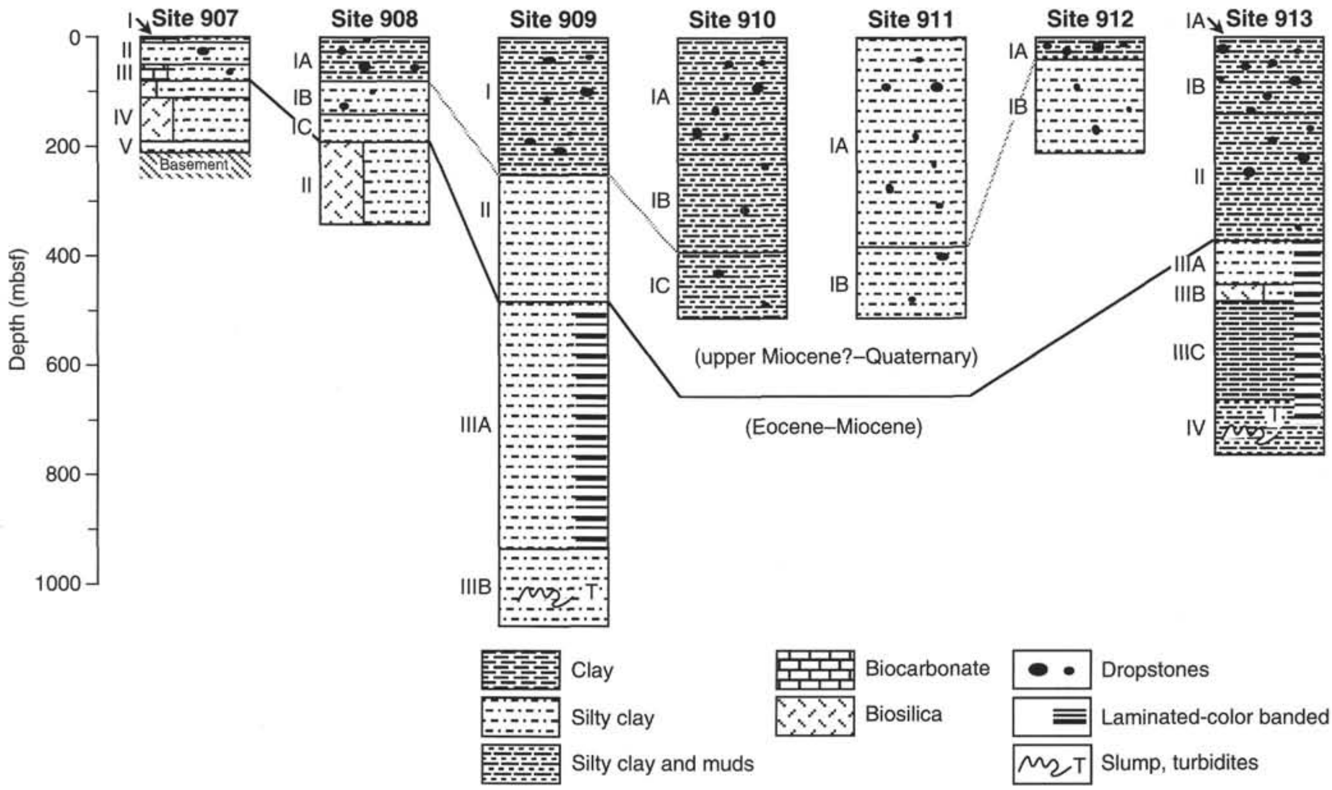

Figure 2. Lithologic summary of Leg 151 drill sites, showing lithologic units.

I (0–16.8 mbsf), consists of bioturbated Quaternary clayey silts, silty clays, and foraminifer-bearing silty muds with minor amounts of biosilica, and silty carbonate ooze. Dropstones or ice-rafted debris (IRD) ≥1 cm are rare. Unit II (16.8–56.3 mbsf) consists of Pliocene to Quaternary massive clayey silts and silty clays, with no biogenic carbonate. Volcanic glass is rare. Unit III (56.3–118.1 mbsf) consists of bioturbated upper Miocene to Pliocene clayey silts and silty clays with biogenic silica, an increase in volcanic glass content, and a decrease in quartz and feldspar content. Dropstones are found throughout. Subunit IIIA has interbedded nannofossil ooze and nannofossil silty clay, whereas Subunit IIIB does not. Unit IV (118.1–197.3 mbsf) consists of bioturbated middle to upper Miocene ash- and biosilica-bearing silty clays and clayey silts, with greenish gray color bands throughout the unit. Abundant, often graded ash layers (from 1 to 15 cm thick) are common in the upper part. Unit V (197.3–216.3 mbsf) consists of bioturbated middle Miocene clayey mud and silty clay, which has high quartz and clay contents and low biosilica content. Volcanic glass commonly fills burrows.

The sedimentary sequence rests on top of acoustic basement consisting of pillow basalts. Bio- and magnetostratigraphy indicate steady sedimentation since the middle Miocene (Chron C5AD) and sedimentation rates range between 10 m/m.y. and 40 m/m.y. The Miocene to middle Pliocene is rich in siliceous microfossils, indicating a time of high productivity. Calcareous microplankton, however, occurs only sporadically from the upper Miocene to Quaternary.

Shipboard physical property measurements and logging establish the cyclic nature of most of the sedimentary column. Extraordinarily high heat flow values and an anomalous alkalinity profile point to the unexpected existence of hydrothermal fluid flow through the deeper part of the sequence.

Site 908

Site 908, on Hovgaard Ridge, was APC/XCB cored to 344.6 mbsf. The logging program was limited because of poor hole quality, including rapid swelling of formations near the unconformity at 185 mbsf.

Two major lithologic units are distinguished (Figs. 2 and 4): Unit I (0–185 mbsf, Pliocene to Quaternary) consists entirely of clayey and silty muds to silty clays, except for a few intervals of foraminifer-bearing clayey or silty mud, which occur in the two uppermost cores, and three distinct ash-layers. Three subunits are distinguished based on dropstone occurrence (mainly clastic sedimentary rocks), texture, and sedimentary structures. The Pliocene and Quaternary sediments represent a dominantly glacial depositional regime, with rare appearances of glacial and interglacial faunas and floras. The entire section is also rich in terrestrial organic material. Unit II (185–344.6 mbsf, upper Oligocene to possibly lower Miocene) consists of bioturbated, biosilica-rich, silty clays with abundant diatoms and common radiolarians and sponge spicules. According to the seismic reflection profile, an angular unconformity separates Units I and II.

Sedimentation rates in the Oligocene sequence may reach 270 m/m.y., indicating very high productivity during that time. Benthic foraminifers indicate a deep neritic to bathyal paleoenvironment.

Site 909

Site 909 is located on the deep sill in Fram Strait. Holes 909A (0–92.5 mbsf) and 909B (0–135.1 mbsf) were APC cored, whereas Hole 909C was RCB cored, penetrating to 1061.8 mbsf. Hole 909C deviated by up to 25.6° from the vertical at depth.

Three lithologic units are defined (Figs. 2 and 5): Unit I (0–248.8 mbsf, Pliocene to Quaternary) consists of color-banded, interbedded clays, silty clays, and clayey muds with varying amounts of dropstones (down to 240 mbsf) and monosulfides. Dropstones are mostly clastic sedimentary and crystalline rocks, rarely limestones. Coal fragments occur in many horizons. The upper 50 m contains minor occurrences of calcareous nannofossils. Unit II (248.8–518.3 mbsf, Miocene to Pliocene) consists of variably bioturbated and color banded silty clays and clayey silts, increasingly fissile downhole, and con-

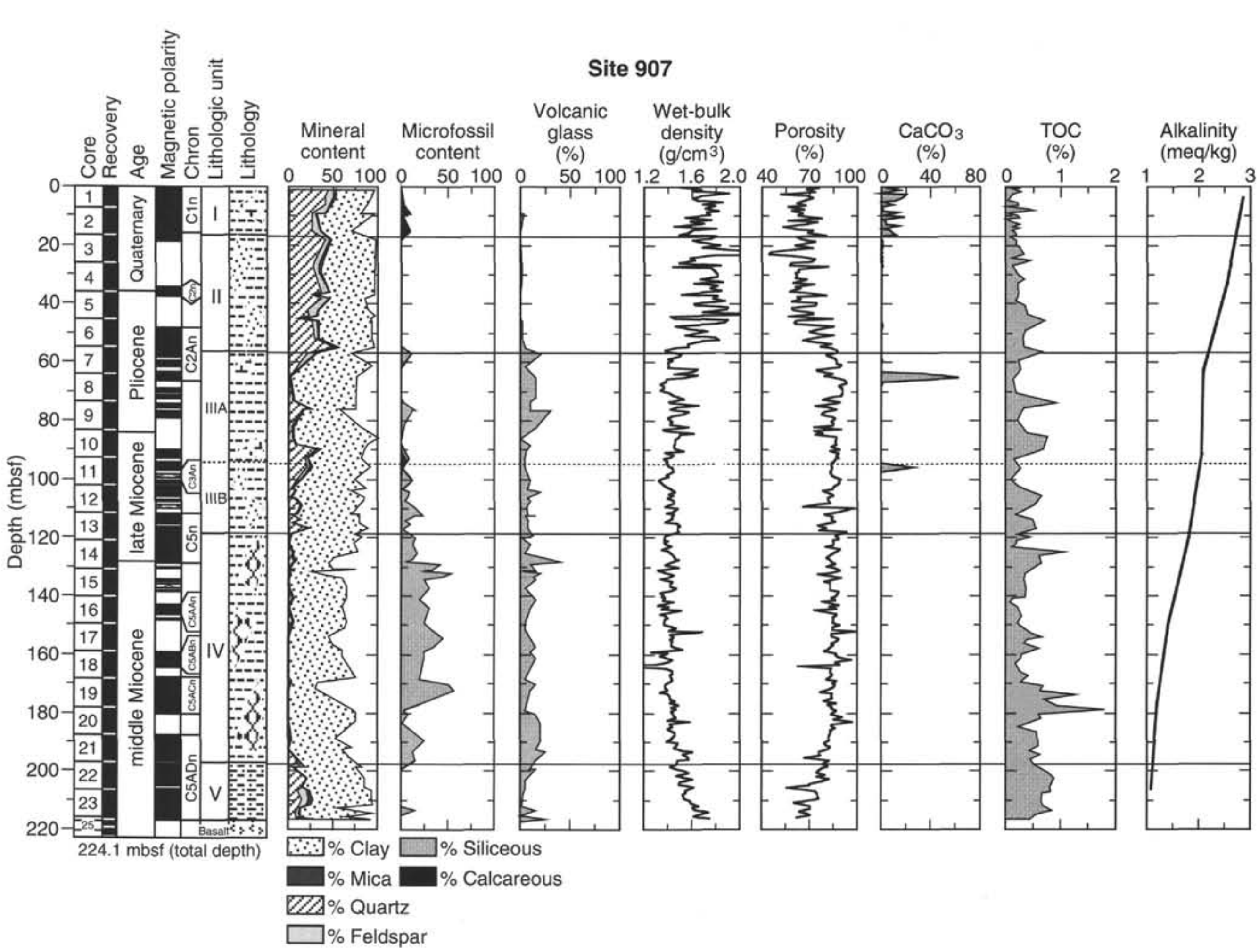

Figure 3. Geologic summary of Site 907, showing core recovery, age, magnetic polarity, lithologic units, sedimentary components, physical properties, percent carbonate and total organic carbon (TOC), and pore-water alkalinity.

tains common pyrite. Some clays are carbonate-rich. Bioturbation is light to moderate throughout. Iron-sulfide concretions and diffuse pods are few. Subunit IIIA (518.3–923.4 mbsf) consists of dark gray silty clays, clayey silts and muds, sometimes carbonate-bearing, and has meter-scale intervals of bioturbated layers and laminations. Subunit IIIB (923.4–1061.8 mbsf) consists of dark gray silty clays, clayey silts, clayey and silty muds, which have several intervals of folded and otherwise deformed bedding. Disseminated pyrite, glauconite, and agglutinated benthic foraminifers are common.

Fossil assemblages consist mostly of palynomorphs as well as agglutinated benthic foraminifers. Dinoflagellates suggest a nearly complete Miocene section. Rare calcareous nannofossils at the base of the hole give an age of latest Oligocene to early Miocene. Benthic foraminifers, however, suggest an older age (early to late Oligocene), indicating unusual diachrony of this group, possibly related to the migration of benthic habitats. Siliceous microfossils are virtually absent, but dissolved silica in pore waters in the upper part of the section is high enough to suggest their original presence. In the lower part of the section, dissolved silica is so low that the original sediments must have been opal-free.

The paleomagnetic record is good in the Pliocene and Quaternary, and sedimentation rates of 50–80 m/m.y. are suggested for the upper 400 mbsf. Below this level, the magnetostratigraphy is problematic.

Gas disruption is severe in the upper part of the section. Organic carbon values are relatively high throughout, with maximum values of 1.5%–2.6% in the lowermost 60 m of the site. Minor amounts of heavier hydrocarbons first occur downhole at about 440 mbsf, and show a drastic two-step increase in propane, butanes, pentanes, and hexanes at about 1020 and 1050 mbsf, as well as the occurrence of strong, light-yellow fluorescence in the lowermost two cores.

Despite high gas concentrations, a good-quality data set of physical properties has been obtained. Compaction effects are not complete even at the base of Hole 909C. Physical property profiles are marked by abrupt increases, as bulk density values increase over very short depth intervals, often coinciding with lithostratigraphic boundaries. Physical property measurements were supported by a successful logging program. The average velocity in Hole 909C was 2.02 km/s. The total depth of penetration in Hole 909C is equivalent to 1.023 s TWT. The acoustic basement reflector is probably about 140 m below the terminal depth.

Site 910

Site 910, located on the central portion of the inner Yermak Plateau, serves as the shallow water member of a bathymetric transect. Very stiff and sticky surface sediments inhibited APC and XCB coring and recovery, whereas RCB coring improved recovery only below 150 mbsf.

One lithologic unit is distinguished that contains very firm, nearly homogeneous silty clays and clayey silts, highly consolidated in the

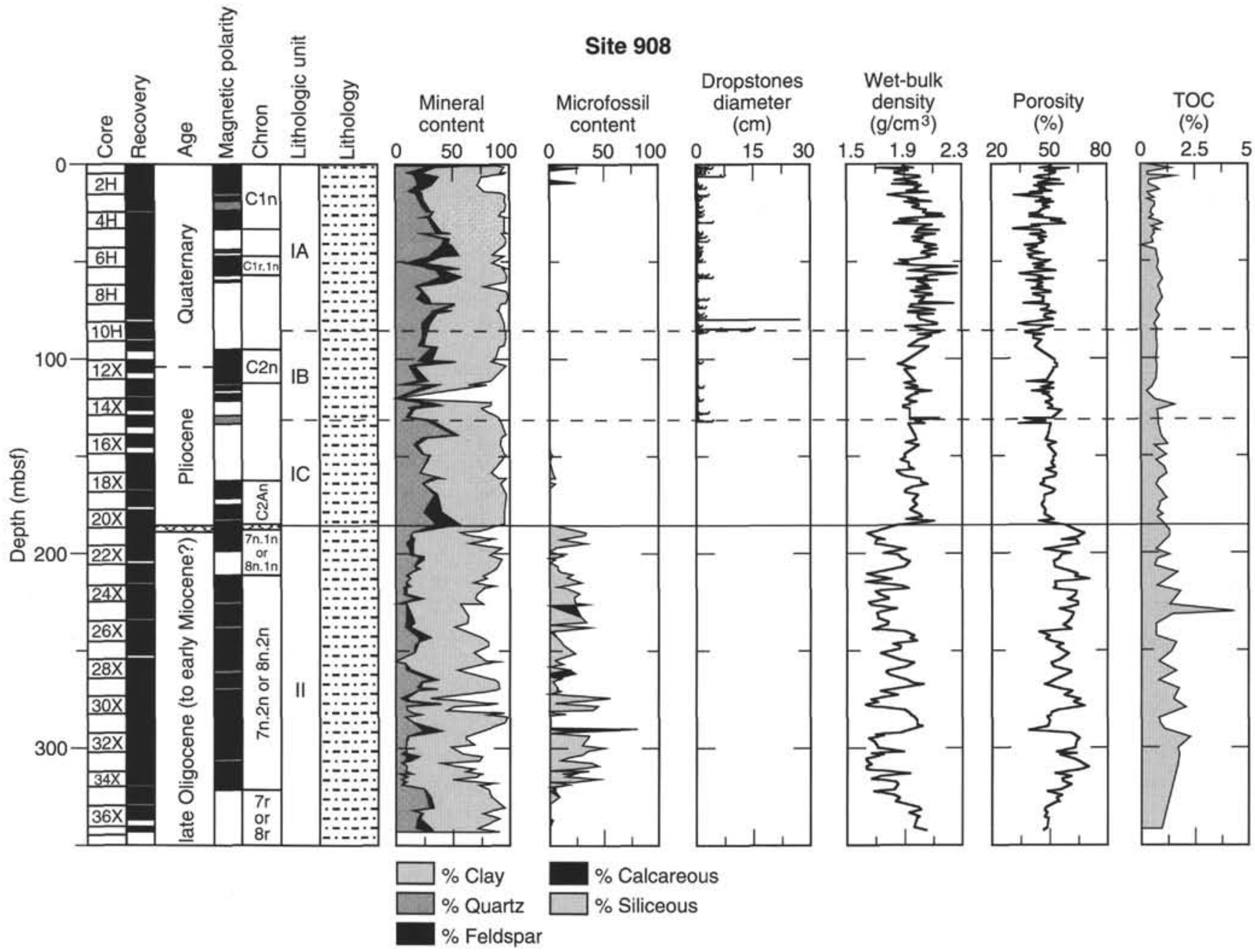

Figure 4. Geologic summary of Site 908, showing core recovery, age, magnetic polarity, lithologic units, sedimentary components, physical properties, and percent total organic carbon (TOC).

surface layers (Figs. 2 and 6). Dropstones are common down to 208.7 mbsf and scarcer below this. Three subunits are distinguished based on dropstone frequency and variations in siliciclastic abundance. Reworked siliceous microfossils, episodic occurrences of mollusc fragments, and wood fragments occur in some intervals. Carbonate values are low (between 1.5% and 6%), and organic carbon values are relatively high throughout (0.7%–1.4%).

Calcareous nannofossils and planktonic foraminifers occur sporadically, but indicate a Quaternary age in the upper 60–100 mbsf, and an extended Pliocene sequence down to 507.4 mbsf. Benthic foraminifers are present throughout, and provide a basis for ecologic and oceanographic interpretations of the bottom conditions. Benthic foraminifers suggest a Pacific influence below 360 mbsf, and also indicate a deepening of the shelf environment with depth in hole. Terrestrial plant material and palynomorphs are common throughout the section, whereas siliceous microfossils are almost absent. Silica in the interstitial waters is substantially lower than at other sites, which appears to reflect equilibrium with diagenetic opal phases. Magnetostratigraphy is poor, in part owing to poor recovery in much of the section.

Methane contents were high throughout (10,000–100,000 ppm, based on headspace). Significant amounts of ethane and propane occurred below 300 mbsf. Physical properties indicate that the upper part of the sequence is highly overconsolidated. Two geotechnical units are recognized, based on the marked increase in shear strength observed at 18 mbsf in Holes 910A and 910C. Sharp increases in sediment strength (from <100 kPa to >300 kPa) and wet-bulk density (from 1.7 g/cm^3 to 2.2 g/cm^3), and a sharp decrease in porosity (from 50% to 35%) between 0 and 20 mbsf indicates that the shallow sediments are overconsolidated. Below 150 mbsf, where core recovery is better, the sediments show more normal distributions of index properties and strength. The overconsolidation of shallow sediments of this site may result from ice-loading. Hole 910D is dedicated as a geotechnical hole to investigate in-situ properties of the overconsolidated glacial Quaternary and Pliocene sediments.

Site 911

Site 911 is located in the shallow southern part of the Yermak Plateau, at a moderate distance Northeast of Site 910. Three holes were drilled, the first to a maximum depth of 505.8 mbsf. A single lithologic unit is defined in all three holes, consisting of Quaternary and Pliocene, variably bioturbated, unlithified, homogeneous clayey silts and silty clays, with minor layers of silty and clayey mud (Figs. 2 and 7). Biogenic particles are rare. Slight to intense bioturbation is present throughout the sequence. Dropstones are more common above 380.4 mbsf and less common below, marking the boundary between two subunits. Dominant dropstone lithologies are siltstones, sandstones, and shales; minor lithologies are coal fragments, plutonic rocks, and limestones.

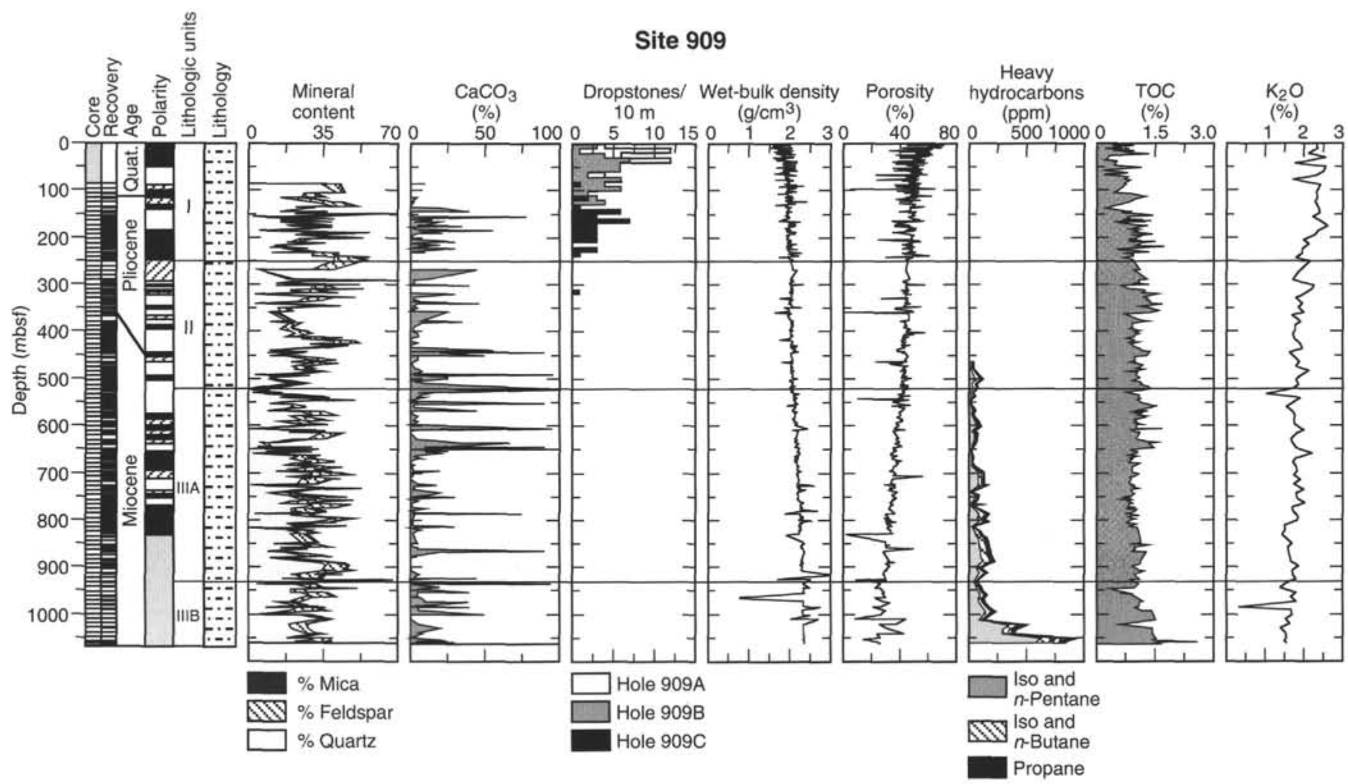

Figure 5. Geologic summary of Site 909, showing core recovery, age, magnetic polarity, lithologic units, sedimentary components, physical properties, and heavy hydrocarbon content, percent total organic carbon (TOC), and percent K_2O.

Site 911 contains rare to common Quaternary and Pliocene benthic and planktonic foraminifers and calcareous nannofossils; siliceous microfossils are absent with the exception of rare recrystallized and reworked specimens. The Brunhes, Matuyama, and Gauss chrons, as well as the Jaramillo and Olduvai subchrons are well defined at this site, and the Emperor and Cobb Mountain Events are tentatively identified. The Quaternary/Pliocene boundary is at about 240 mbsf, and sedimentation rates range from 170 m/m.y. in the Pliocene and pre-Jaramillo, to about 100 m/m.y. during the last million years.

Downhole logs indicate no major downhole lithologic trends, but some do exhibit a cyclic nature. Preliminary spectral analyses define spectral power in the 40-k.y. and 100-k.y. bands, reflecting known Milankovitch frequencies.

Relatively severe gas- and drilling-induced disturbances occur in the deep parts of the section. Five geotechnical units are defined, mainly reflecting downcore variability of bulk densities. Sediments in the top 50 m show some evidence for overcompaction, similar to, but of less magnitude than, those at Site 910.

The concentrations of headspace methane are high throughout the sedimentary section, ranging from 8000 to 80,000 ppm.

Site 912

Site 912 is located on the southwestern edge of the Yermak Plateau and is an intermediate member of a depth transect. Hole 912A reached 145.4 mbsf, Hole 912B only 40.5 mbsf, and Hole 912C reached 209.1 mbsf.

A single lithologic unit (Figs. 2 and 8), contains Pliocene to Quaternary, unlithified, slightly to moderately bioturbated silty clays and clayey silts, with faint color banding, and higher dropstone abundances than at Sites 910 and 911. Dropstones are dominantly silt-, sand-, and mudstones, with common metamorphic and igneous rocks as well. An uphole increase in dropstone abundance at 40 mbsf delineates the two subunits. The sediments suggest a hemipelagic, glaciomarine depositional environment.

All three holes recovered a Quaternary and Pliocene sequence of ice-rafted sediments with scattered occurrences of calcareous microfossils. Siliceous microfossils are absent, with the exception of rare reworked diatoms and silicoflagellates, rare and poorly preserved radiolarians, and rare diatoms indicative of uppermost Pliocene to lower upper Quaternary. Dinoflagellates are rare and non-age-diagnostic; terrestrial palynomorphs are common throughout. Ice-rafted *Inoceramus* prisms are found in Pliocene sediments.

The magnetostratigraphic results are consistent with biostratigraphic age determinations. Because of poor core recovery it was not possible to estimate Pliocene sedimentation rates. Pre-Jaramillo sedimentation rates vary from 80 to 100 m/m.y., but they decrease to about 30 m/m.y. during the last 1 m.y. of deposition.

Physical properties distinguish three geotechnical units: G-I (0–8 mbsf) comprises highly variable, but generally low bulk densities and high porosities; G-II (8–50 mbsf) consists of highly variable bulk densities and inversely related trends in water content and porosity; in G-III (below 50 mbsf) recovery is reduced, but physical properties appear more constant.

Site 913

Site 913 is located in the deep Greenland Basin on crust slightly older than magnetic Chron C24n.3n. Hole 913A was APC/XCB cored to 103.6 mbsf; Hole 913B was RCB and wash cored from 86.0 to 770.3 mbsf. A very high abundance of dropstones, as well as gravel and sandy layers, caused very low recovery in the upper 423 mbsf.

Sediments in Hole 913A and the shallow part of Hole 913B (to 307.2 mbsf) are in large part glacially influenced. They consist of massive, interbedded lithologies with a variety of textures, from clay to silty clay and clayey mud to silty sand, with common gravel and sandy layers, 2%–6% carbonate and 0.1%–1% organic carbon (Fig.

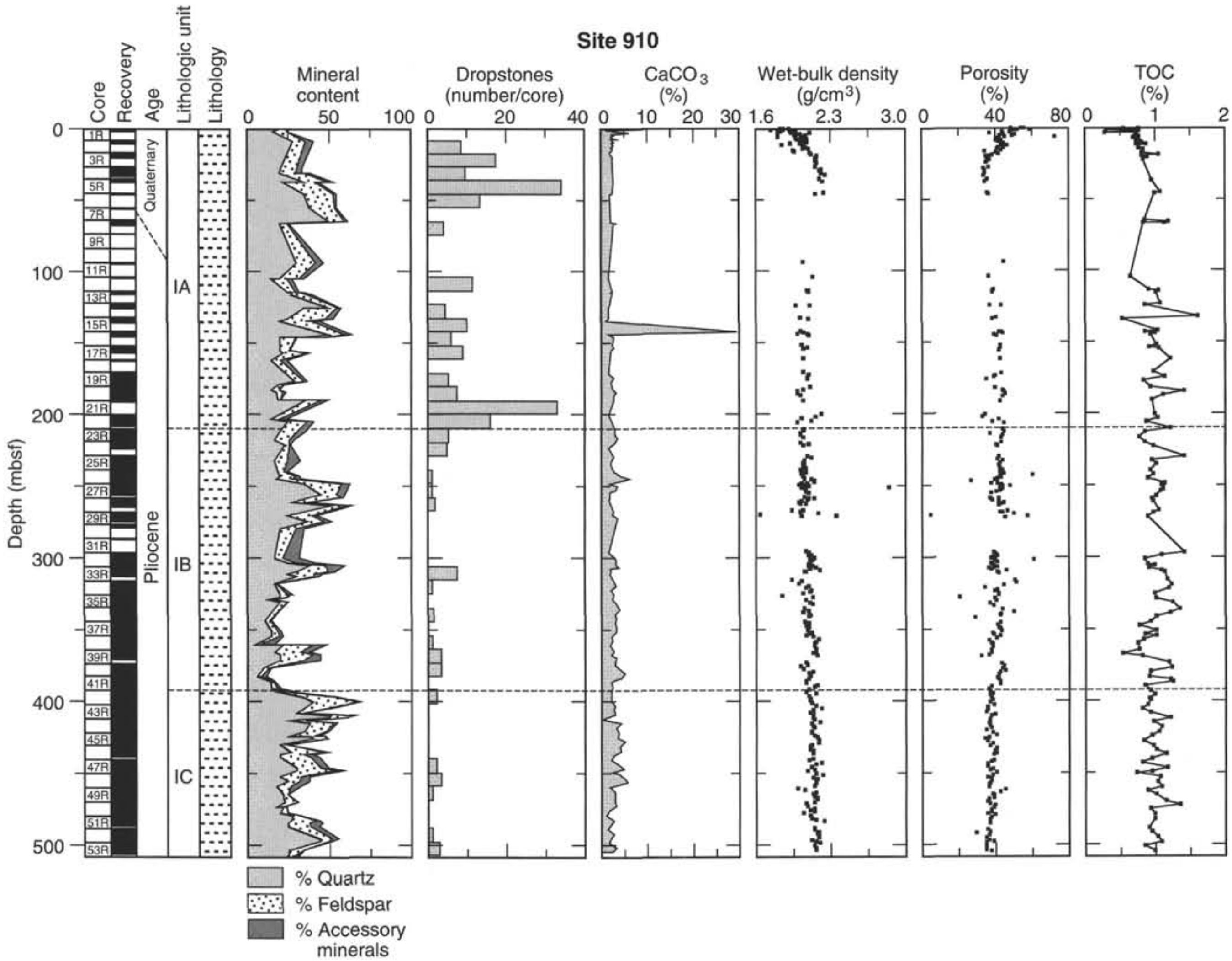

Figure 6. Geologic summary of Site 910, showing core recovery, age, lithologic units, sedimentary components, physical properties, and percent total organic carbon (TOC).

9). Dropstones are particularly prevalent in the upper 131 mbsf (some large ones were actually cored by the RCB), and include sedimentary (quartz sand-, silt-, and limestones), igneous (gabbros, granites), and metamorphic (quartzites, amphibolites, gneisses, schists) lithologies. Crystalline rocks are predominant, in contrast with the Yermak Plateau and Fram Strait sites, where fine-grained clastic sedimentary rocks are most common. Siliciclastics dominate the shallow sediments, but planktonic and benthic foraminifers compose up to 40% of specific layers, and nannofossils are a trace component.

Siliciclastics are still present in sediments recovered from below 435 mbsf, but are not dominant. Carbonate values are usually <1%; only in selected thin horizons do they rise to 10%–23%. Organic carbon concentrations reach only 0.1%–0.5% (the exception being a value of 2.7% in Core 151-913B-27R). Alteration products such as zeolites are more important, as are siliceous microfossils. Perhaps the most distinctive aspect of the deeper sediments is their riotous color schemes: a full palette of greens characterizes the highly bioturbated zones, whereas laminated intervals show a full range of greens mixed with a stunning array of vivid blues, browns, violets, tans, and yellows.

Four lithologic units are defined (Figs. 2 and 9): Unit I is divided into two subunits (0–143.8 mbsf). Subunit IA (0–3.2 mbsf, Quaternary) consists of interbedded clays, silts and sand, biogenic-bearing clay and silty mud. There are few dropstones. Subunit IB (3.2–143.8 mbsf, Quaternary) consists of interbedded clayey mud and silty mud with minor gravelly or gravel-bearing layers, defined by the presence of abundant large dropstones of various lithologies. Subunit II (143.8–378.7 mbsf, middle Miocene to Pliocene) is predominantly composed of silty clay, with clayey silt, silty mud, and very few dropstones. Unit III (378.7–770.3 mbsf) is subdivided into three subunits. Subunit IIIA (378.7–462.0 mbsf, late Eocene to middle Miocene) consists of interbedded, massive and laminated silty clay and clay, which at intervals is slightly bioturbated and can contain Mn-concretions. Subunit IIIB (462.0–500.3 mbsf, late Eocene to early Oligocene) contains biosilica-bearing clay, biosiliceous clay to silty clay, clayey and silty siliceous ooze with layers of dusky to bright greens, blues and purples. Diatoms and radiolarians both occur in concentrations as great as 20%. Subunit IIIC (500.3–674.1 mbsf, middle Eocene to early Oligocene) consists of massive and laminated clays, minor silty clays, and muds containing rare microfossils. Unit IV (674.1–770.3 mbsf, middle Eocene) is composed of laminated clays, silty clays, and massive silty clays, as well as clayey and silty muds in fining upward sequences. In the lower part, some layers of well-cemented calcareous sandstones and siltstones occur.

Planktonic and benthic foraminifers as well as nannofossils give a Quaternary to Pliocene age to the top 288.4 mbsf. From 288.4 to

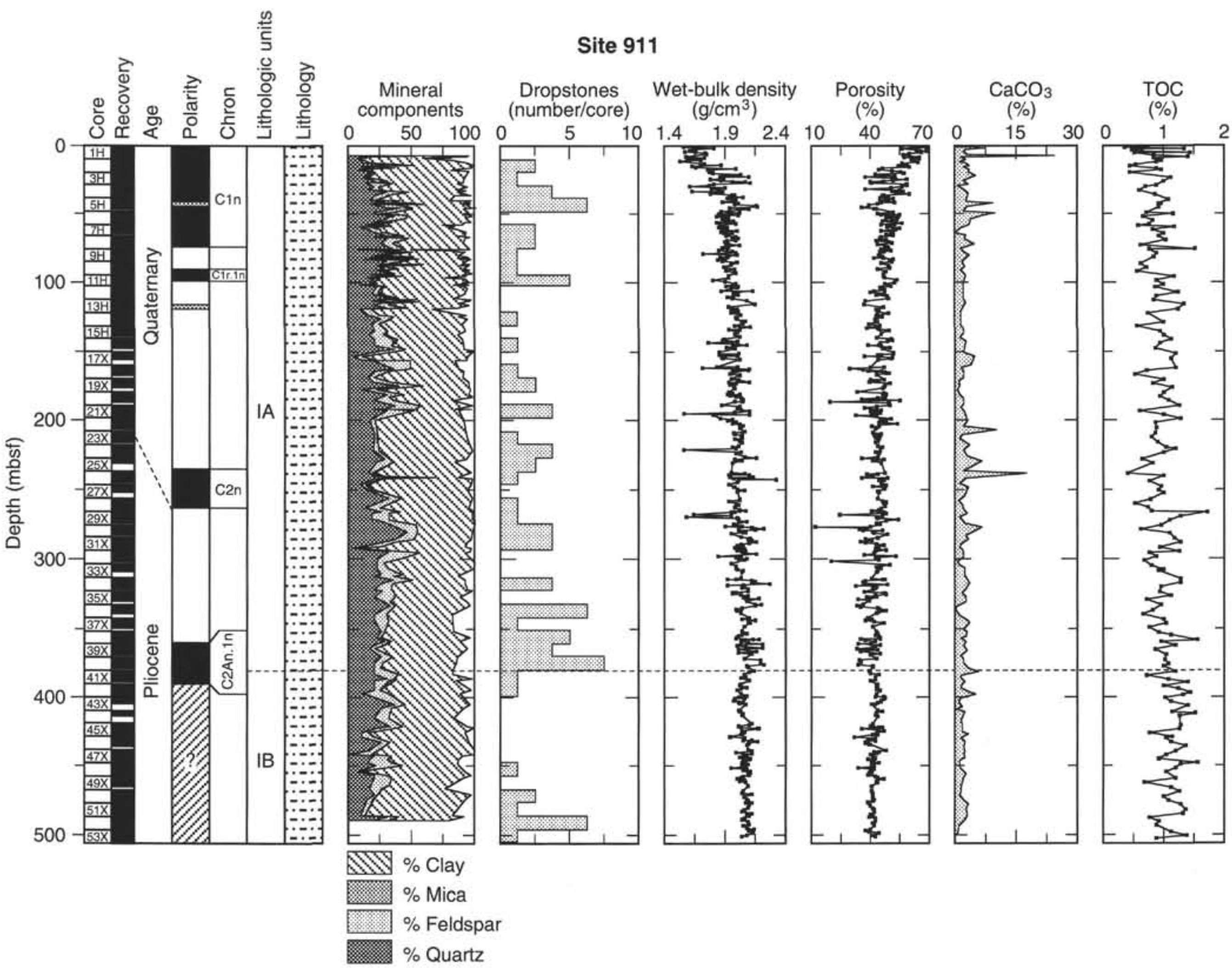

Figure 7. Geologic summary of Site 911, showing core recovery, age, magnetic polarity, lithologic units, sedimentary components, physical properties, and percent carbonate and total organic carbon (TOC).

375.2 mbsf, sediments are either barren of microfossils or of indeterminate age due to poor recovery. Diatoms, radiolarians, and benthic foraminifers recovered at 423.5 mbsf indicate an age of middle to early late Miocene for the overlying washed section.

Sediments at 471.6 to 490.7 mbsf contain lower Oligocene to upper Eocene radiolarians, diatoms, and benthic foraminifers; radiolarians and diatoms are particularly well preserved and abundant through the upper part of this interval. Diatoms are absent with the exception of pyritized forms at 558.1 mbsf. Radiolarians abundances are reduced, but continuous from 490.7 to 558.1 mbsf, and co-occur with sporadic appearances of *Bolboforma*, planktonic and benthic foraminifers. Sediments from 500.3 mbsf to the base of the hole are of middle to late Eocene age, based on agglutinated benthic foraminifers and *Bolboforma*. Shipboard magnetostratigraphic studies are inconclusive because of poor recovery and very low NRM intensities.

Bulk densities from the glacial marine sediments range from 1.95 to 2.1 g/cm^3 in the upper 400 mbsf, but decrease to 1.8–1.45 g/cm^3 as sediments become finely laminated farther below and the siliceous microfossil component increases. Velocities measured from this laminated interval show typical thin-bedded anisotropic behavior (12% *P*-wave anisotropy). Along the bedding planes the velocities are 1750 m/s. The lowered density in the biosiliceous material relative to the glacial marine sediments may partially explain the increased velocities.

Table 1, at the end of this chapter, summarizes the drilling results for Sites 907–913.

THEMATIC DRILLING RESULTS

Physical Properties

Leg 151 sediments generally consist of sequences of fairly homogeneous hemipelagic sediments without turbidites and other features indicative of abrupt sedimentary events. They offer the possibility of recognizing the effects of long-term consolidation on physical properties as well as more subtle changes in hemipelagic sedimentation induced by Pliocene-Quaternary climatic cyclicity. The variation in physical properties at the sites was of three main types:

1. Long-term trends in parameters such as bulk density and porosity, related to processes of sediment consolidation, and to major changes in sediment composition (terrigenous:biogenic ratio). These result from major shifts in climate boundary conditions like the initiation and intensification of major Northern Hemisphere glaciation. The large, sustained increase in bulk density at ca. 2.5 Ma at Site 907 is an example of the latter effect.

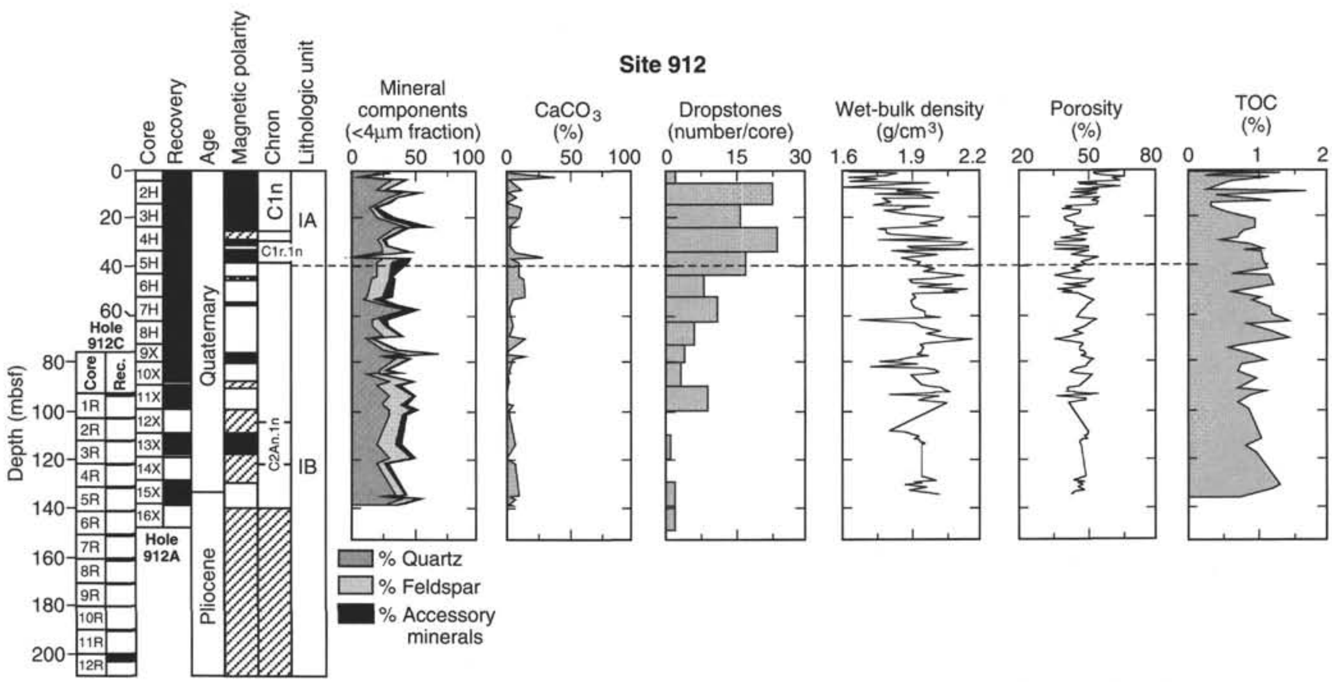

Figure 8. Geologic summary of Site 912, showing core recovery, age, magnetic polarity, lithologic units, sedimentary components, physical properties, and percent total organic carbon (TOC).

2. Rhythmical changes on Earth orbital time scales produced by the effects of variations in, for example, ice-rafting intensity, proximity to ice margins, current activity, and biological productivity on sediment composition and grain size. These features are most recognizable in the Pliocene-Quaternary glacial sediments; however, they are not confined to them, occurring in, for instance, the upper Oligocene at Site 908. The most consistent periodicity in space and time at the Leg 151 sites is 41 k.y.: most of the variance in GRAPE density in the post 2.4 Ma interval at Site 907 occurs at this periodicity.
3. Sites 910 and 911 have overconsolidated intervals at shallow depths.

Iceland Plateau—Site 907

Relatively low and constant bulk densities shifted abruptly to more variable but consistently higher bulk densities at ca. 2.5 Ma (Fig. 10). The shift corresponds to a lithologic change from biosiliceous-rich silts and clays with a significant biosiliceous content to pure silts and clays, and is time-correlative with a similar bulk-density increase at Site 642 on the Vøring Plateau.

East Greenland Margin—Site 913

Detailed physical properties measurements are confined to the sub-400-m (Miocene–Eocene) interval (Fig. 10). With the exception of a biosilica-rich low-density interval centered on 475 mbsf, the sequence of clay and silty mud shows a standard consolidation profile of gradually increasing bulk density with depth.

Fram Strait—Sites 908, 909

Bulk densities in the Pliocene–Quaternary sequence at Site 908 show high frequency (Earth orbital time scale) fluctuations (Fig. 10). The marked increase in bulk density with depth usually associated with normal consolidation is absent. This may be related to core disturbance by gas expansion. Bulk densities in the upper Oligocene section show a pattern of high frequency fluctuations that result from the alternation of silty clay and biosilica-rich layers. Site 909 has a characteristic consolidation profile for relatively homogeneous marine siliciclastic sediments—bulk density increases rapidly (over the upper several tens of meters) and then more slowly with depth from ca. 1.6 g/cm^3 at the surface to ca. 2.4 g/cm^3 at ca. 1000 m (Fig. 10). However, even at this depth the bulk density fails to approach a constant value, differing from most of the Leg 151 sites where the compaction gradients are smaller.

Yermak Plateau—Sites 910, 911, and 912

At Site 910 the uppermost 18 mbsf shows a pattern of steeply rising bulk density (from 1.4 to over 2.0 g/cm^3; Fig. 10) and a sharp increase in shear strength at the base of this interval, unusual features for such shallow burial depths. The highest bulk densities obtained at this site (ca. 2.25 g/cm^3) occur between 35 and 40 mbsf. Below this, the bulk density profile reverses, with values decreasing toward the base of the profile. The entire bulk density profile is well above the expected values for the consolidation of terrigenous silty clay, suggesting that these sediments may have been subjected to a much greater overburden pressure in the past, perhaps due to ice loading.

At Site 911, physical properties reflect the gradual compactive dewatering of sediments (Fig. 10). A surficial sediment layer of relatively high water content and variable physical properties grades slowly into a layer that exhibits more uniform physical properties below 400 mbsf.

At Site 912, a surficial (ca. 10 m) sediment layer with highly variable but generally low bulk densities and high porosities overlies a zone of silty clays and muds having variable amounts of dropstones and increased but again highly variable bulk densities (Fig. 10).

Logging

The results summarized here are from analysis of the raw logging data. Much of the log data (especially the FMS and geochemical data, which are not discussed here) require post-cruise processing to re-

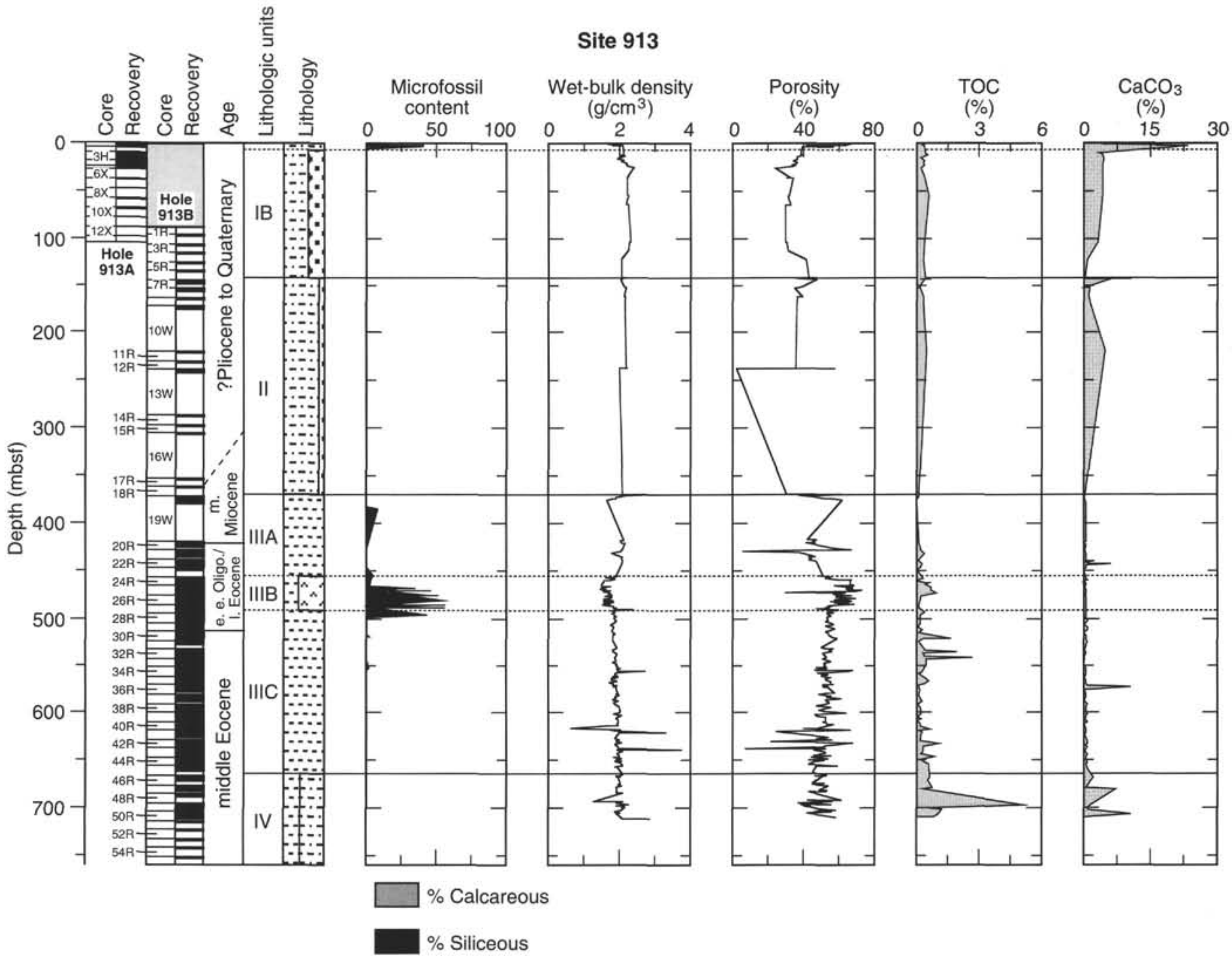

Figure 9. Geologic summary of Site 913, showing core recovery, age, lithologic units, microfossil content, physical properties, and percent total organic carbon (TOC) and carbonate.

move artifacts caused by environmental factors such as borehole size, before detailed analysis can be performed.

Downhole logs were obtained from Hole 907A on the Iceland Plateau, Holes 908A and 909C in the Fram Strait, and Holes 910C and 911A on the Yermak Plateau. The logged interval in Hole 907A covering the middle Miocene to lower Pliocene sediments of lithologic Units III and IV (Fig. 2) is predominantly clay but with a significant biosilica content. This distinguishes it from the other logged holes as the higher opaline content results in very high log porosities of 75%–80%, reflected in the low resistivity and density readings and the relatively low gamma-ray in comparison to the other logged sites.

The most prominent feature of Site 908 is an angular unconformity visible on seismic records, occurring at 185 mbsf, a feature well defined in all of the logging data. The Pliocene sequence above the unconformity is predominantly clay along with quartz and feldspar with log porosities of ~50% and average bulk densities of ~1.85 g/cm^3. The upper Pliocene sequence has a very well defined cyclic nature best exhibited in the resistivity. Post-cruise analysis will test whether this is of Milankovitch frequencies. Lithologic Unit II below the unconformity is characterized by higher log porosity (60%) and lower bulk density and gamma-ray counts, owing to the presence of a significant biosiliceous component in this upper Oligocene sequence.

The logged section of Hole 909C covers almost the entire drilled sequence at this hole, representing an upper Oligocene/lower Miocene to Quaternary sequence. The lithology is dominated by clay and exhibits no major variation downhole. Sonic velocity shows a remarkably linear trend with velocities of 1.5 km/s at the top to 2.6 km/s at 1010 mbsf. Log porosities show a similar trend with a range of 45% to 30% from the top to the bottom of the hole. The FMS shows disturbed beds, interpreted as slumping, in the intervals 1005–998 mbsf and 966–959 mbsf within Subunit IIB, corresponding well with the lithologic descriptions of core material. Post-cruise processing of the images will yield enhanced delineation of the slumps as well as directional information. The FMS also showed the deviation of the hole from vertical increased from about 13° at 590 mbsf to 25.6° at the base of hole in a northeasterly direction, perhaps following the direction of minimum stress within the sediments.

Hole 910C suffered from poor core recovery (57.8% overall) and the logging data provide valuable information for several intervals of very poor recovery. The Pliocene sequence covered by the logs is dominated by clay with subordinate quartz and feldspar. The total gamma-ray is high as a result. Log porosity is fairly constant (45%) downhole and velocity increases fairly linearly with depth, although jumps in the bottom part of the hole are noted where larger quartz and feldspar abundances are present in the core material.

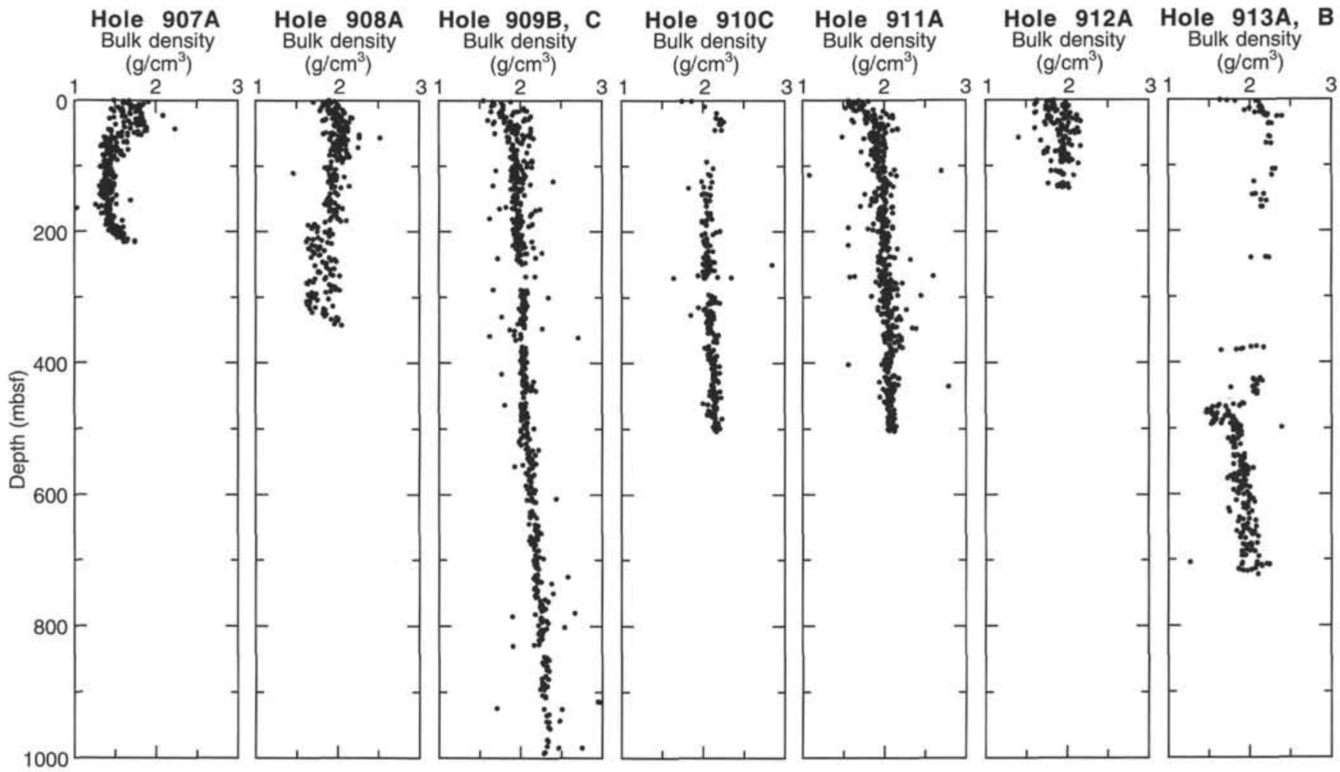

Figure 10. Comparison of bulk density profiles (discrete measurements) from Sites 907 through 913.

Logging data provided comprehensive coverage of Hole 911A. The Pliocene to Quaternary sequence is again dominated by an unlithified dark gray silty clay lithology. The logs exhibit no major variations downhole, reflecting the homogenous nature of the sediment. Log porosity is a fairly constant 50% downhole, and log velocity increases linearly from 1.6 to 1.9 km/s from 110 to 460 mbsf. Iron sulfide nodules were detected throughout the hole, usually filling burrows. The highly conductive nature of these nodules causes low spikes in the microresistivity data of the FMS, despite their small size (0.5–2 cm). Post-cruise study of the FMS data should enable a more accurate delineation of the abundance of these nodules in the hole.

Despite the lack of major trends, the logs at Hole 911A exhibit marked cyclicity in the resistivity data. Preliminary spectral analysis suggests it to be of Milankovitch frequencies. At Site 911 the sedimentation rates are particularly high, reaching 193 m/m.y. as calculated from the preliminary paleomagnetic constraints, yielding a temporal resolution in the logs on the order of 1 k.y. Preliminary spectral analyses over the interval 1.1–1.8 Ma (~110–240 mbsf) show strong spectral power at ~40 k.y. and to a lesser extent 100 k.y. The dominant 40-k.y. peak is probably a climatic expression of the 41-k.y. orbital obliquity cycle. It is uncertain what the cyclicity represents in terms of varying physical components in the formation. Resistivity is proportional to the inverse square of porosity (Archie, 1942), and these porosity changes may relate to grain size variations, which are in turn driven by fluctuations in ice cover. Planned post-cruise work will address this issue.

Inter-site Correlation

Lateral correlation of the logging data among the various drill sites on Leg 151 is difficult at present because of the homogeneous nature of the sediments and the lack of major lithologic variations that can be easily correlated among sites. Much of the log data are also compromised by the often large and variable hole diameter encountered on this leg. These artifacts will be mitigated by post-cruise processing.

Sedimentology and Dropstone Petrography

Sedimentology

The deposition of Leg 151 sediments is mainly controlled by the global paleoclimatic and paleoceanographic environment and the regional tectonic evolution and its feedbacks on the global paleoclimate. The sediments may be characterized as three depositional facies types: (1) ice-house (glacial) facies, (2) transitional (cooling) facies, (3) warm-house (pre-glacial) facies (Fig. 2).

The ice-house facies is present at all seven sites as lithologic Unit I. This sequence reaches a thickness of up to 507 m at the Yermak Plateau. The facies consists primarily of gray to dark gray clays, silty clays and clayey silts, often interbedded with silty and clayey mud. Dropstones of different size and lithology are abundant and reach their highest abundances at the Yermak Plateau sites (Sites 910, 911, 912; Figs. 11 and 12). The sporadic occurrences of reworked biosiliceous microfossils, mollusc fragments (*Inoceramus* prisms) and coal fragments are common throughout this facies. Biogenic particles are generally rare and are limited to planktonic and benthic foraminifers and rare calcareous-nannofossil-rich layers. Contacts between lithologies are commonly gradational. Bioturbation is slight to moderate, and burrows are often filled with black monosulfides or white silt material.

A transitional facies is present at the Fram Strait (Sites 908 and 909), on the East Greenland Margin (Site 913) and on the Iceland Plateau (Site 907). This sequence consists mainly of sediments of lithologic Unit II (Site 907 additionally Unit III) and is characterized by dark grayish brown or dark gray silty clays and clayey silts. Minor amounts of dropstones and a few mud beds occur in this facies. Biogenic carbonates and biosiliceous components (e.g., sponge spicules,

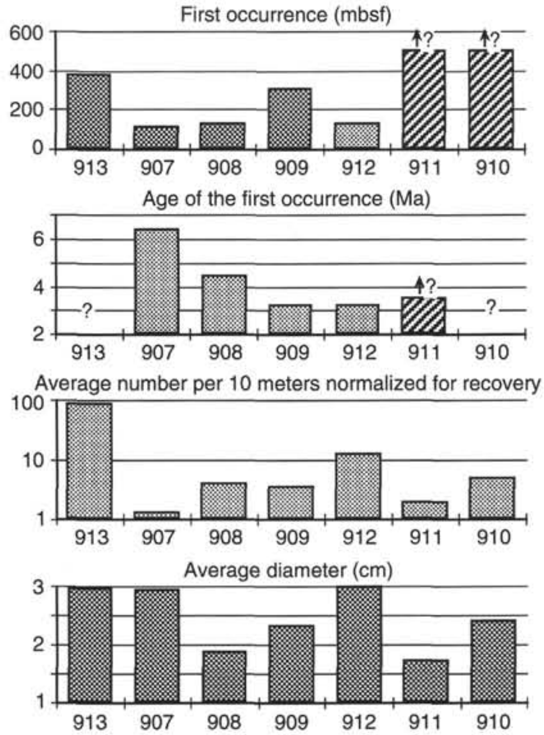

Figure 11. Summary of dropstone occurrences at Sites 907 through 913, showing depth and age of first occurrences, average number per 10 m (normalized for recovery), and average diameter (of dropstones >1 cm).

diatoms, radiolarians) occur in trace quantities. The sediments are commonly moderately bioturbated and massively bedded. Contacts are gradational and often mottled. The transitional facies represents a deterioration of climatic conditions that culminated in the full-blown glaciation evident in the ice-house facies. As such, the two facies contrast in their more or less glacial nature with the clearly nonglacial character of the underlying sediments.

Perhaps the most significant distinction between the glacial and nonglacial facies is the transport mechanism of floating ice. In light of the importance of ice-rafting in the Arctic and subarctic regions considered here, additional discussion is appropriate. Within the ice-rafted detritus carried to the deep sea by icebergs and sea ice, the dropstones found as isolated pebbles in a finer-grained matrix are the most easily identified. Their occurrence, and variations in their abundance and nature, can be used as indicators of glacial conditions.

During Leg 151, dropstones >1 cm in diameter were systematically counted and measured during the visual description of cores (Fig. 11). A number of parameters were derived from these data to compare the distribution of dropstones at different sites. Important variations are evident in the depth of the first (deepest) dropstone occurrence at each site. At Site 907 the first dropstone occurs at 117 mbsf, whereas at Site 913 they appear at 379 mbsf. Deeper first occurrences are found at Sites 910 and 911 on the Yermak Plateau, where dropstones are present to the bottom of all holes. Applying the magnetostratigraphic age models, however, the oldest occurrence of dropstones is observed at Site 907 (6.4 Ma) and the youngest at Site 909 (3.2 Ma). No ages could be assigned to Sites 910 and 913. The occurrence of dropstones as early as the late Miocene is consistent with the general cooling indicated at this time, and with the presence of scarce dropstones in Baffin Bay at 8.5 Ma. However, dropstones are rare throughout Site 907, and icebergs drift over this site under modern interglacial conditions. Thus it is difficult to draw conclusions concerning the development of major ice sheets by the late Miocene.

The number of dropstones, normalized according to recovery and expressed in terms of quantity per 10 m of core (Fig. 12), shows important site-to-site fluctuations. Site 913 is characterized by a very large quantity of dropstones, which contributed to poor recovery (more than 100 dropstones/10 m for relatively full cores and up to 250 dropstones/10 m for the shortest core with matrix-supported pebbles). At Site 907, the number is less than 1 dropstone/10 m. Of the Fram Strait and Yermak Plateau sites, Site 912 has the highest dropstone frequency. There is not a single relationship between abundance of dropstones and distance to glaciated terrains. Dropstone abundance may mainly reflect an iceberg drift pattern similar to today, characterized by restricted influence of the relatively warm Norwegian Current, and by abundant icebergs carried southward in the East Greenland Current.

Abundance of dropstones also varies according to time at all sites. As in most of the DSDP and ODP sites from the North Atlantic, a relative increase in dropstone abundance is observed around 2.5 Ma at Sites 908, 909, 911, and 912 (2.3, 2.5, 2.2, and 2.6 Ma, respectively). No general pattern is observed in younger sediments. However, drop-

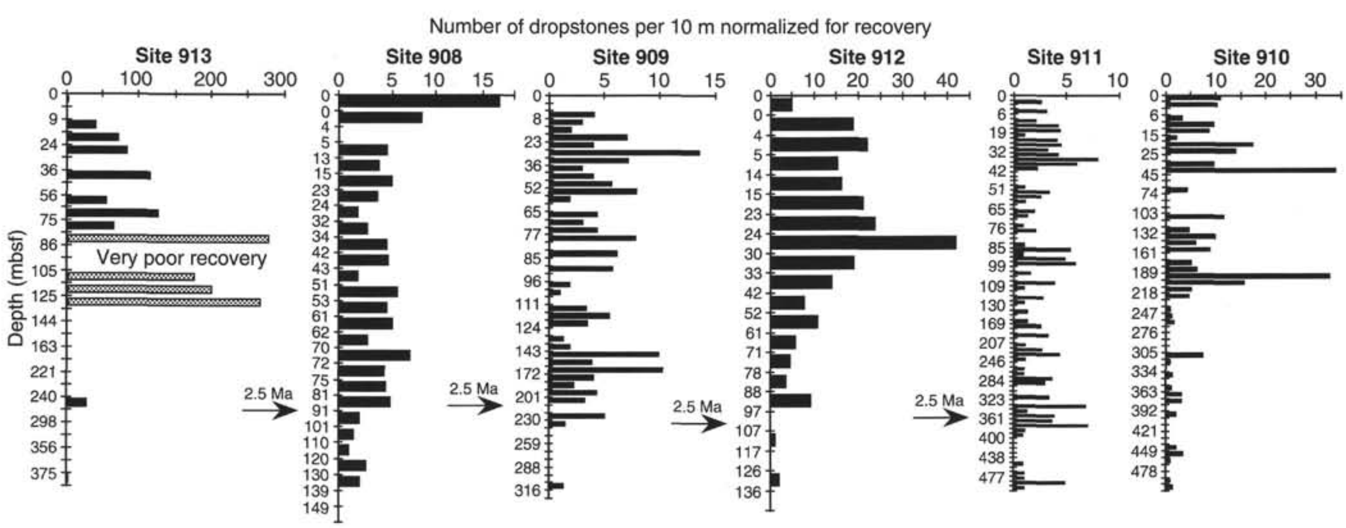

Figure 12. Summary of dropstone abundances (normalized for recovery) vs. depth at Sites 908 through 913.

stone abundances do not seem to fluctuate randomly nor do they increase monotonically. With the exception of Site 908, the number of dropstones generally decreases during the last 0.6–0.8 Ma.

If dropstones provide evidence of ice transport, they nevertheless constitute only a small percentage of the sediment, which is largely dominated by clay- and silt-sized particles. Accumulation rates are high on the Yermak Plateau and the Greenland Margin, and there are few sedimentary structures indicative of downslope transport. Consequently, much of the fine-grained sediment must also be delivered directly by glacier meltwater or carried by icebergs and sea ice.

The warm-house facies is documented in the sediment record of the Fram Strait (Sites 908, 909), the East Greenland Margin (Site 913), and the Iceland Plateau (Site 907), and is characterized by dark greenish gray to dark gray silty clays, clayey silts, and clays. The sediments are generally rich in biosiliceous components such as sponge spicules, diatoms, and radiolarians. In the lower part of this facies biosiliceous components are often replaced by clay aggregates, which could not be further distinguished by smear slide analyses. Thin color bands (≤1 cm) are common at Site 907, whereas the sediments from Sites 908, 909, and 913 are commonly laminated (laminae 1–5 mm). Moderate to intensive bioturbation is present, giving the sediments a mottled appearance and resulting in many gradational color and lithology boundaries.

The fine-grained character of the warm-house sediments is indicative of a lack of ice rafting or a high-energy depositional environment. It is consistent with hemipelagic sedimentation of terrigenous material from suspension. The relatively high sedimentation rates are most likely due to source proximity in the nascent basins. Laminated intervals may relate to the relative restriction of these basins and poor communication with the remainder of the world's deep oceans. Preservation of fine scale layering is at least partially associated with enhanced surface productivity and organic carbon burial, resulting in anoxic bottom water conditions. Spotty recovery, limited correlative intervals, and the poorly constrained origin of the laminae make further interpretation speculative.

Two kinds of sedimentary structures linked to downslope transport occur in the deepest part of Sites 908, 909, and 913. They are limited to rare graded sequences in Site 908, and are more common and well developed in the two other sites. In Site 909, common meter-scale slump structures and rare, well-developed turbidite sequences indicate deformation rather than long downslope transport. In Site 913, well-defined gravity flow deposits occur, changing from massive muds supporting clay clasts to thick homogeneous clay through a laminated silt and clay interval. As they are also associated with distinct changes in sediment texture and composition, they certainly reflect a longer transport from the recently constructed Greenland Margin.

Dropstone Petrography

Determination of the provenance of ice-rafted dropstones can help determine paleo-current patterns, and possibly major changes in current patterns through time (Bischof et al., 1990). Most of the Leg 151 dropstones are nondescript, widespread rock types such as granite, sandstone, and quartzites. Our future shore-based investigations will entail consulting specialists in the local geology of possible source areas (i.e., Norway, Svalbard, Greenland, and the Canadian Arctic Islands) to see if any of the collected dropstones have unique provenances. We will also look at the total assemblage of dropstones from the individual sites (Fig. 13). The dropstone assemblages from sites along the eastern parts of the Fram Strait and the Yermak Plateau, (Sites 908–912) which currently lie beneath the path of the West Spitsbergen Current (Quadfasel et al., 1987), show clear dominance by sedimentary rock types over igneous and metamorphic rock types. Furthermore, coal and other sediments associated with paralic facies are common, especially at Site 908. We suggest that this dropstone assemblage must have been eroded mostly from Svalbard, or perhaps in glacial times from the Norwegian and the Barents shelves, and is a proxy for the West Spitsbergen Current or an earlier current system following roughly the same path (Bischof, 1989).

In contrast, the dropstone assemblage at Site 913, on the East Greenland Margin, is dominated by metamorphic and igneous rocks. This assemblage reflects the influence of the East Greenland Current, carrying icebergs from the northernmost part of Greenland (Clark and Hanson, 1983).

It is interesting that the sites on the Yermak Plateau (Sites 910, 911, and 912) resemble Sites 908 and 909 so much. This suggests that icebergs carried with the inflow of the relatively warm West Spitsbergen Current to the Arctic Ocean (Manley et al., 1992) have been the main source of ice-rafted material in this area.

Inorganic Geochemistry

Two notable geochemical indicators stood out from the bulk sediment XRF studies: silica and potassium. The silica concentration in the detrital fraction of Sites 908 through 913 was virtually invariant at or just above 60 wt%. The silica concentration in the detrital parts of Hole 907A, however, was only about 50%. This low concentration was due, no doubt, to the proximity of volcanic sources, but also suggests either a gradient or, perhaps, a sharp boundary between Site 907 and the rest of the region. This boundary must persist in time and probably moves back and forth in response to volcanic activity, wind, and currents. The history of this boundary and the paleoenvironmental information to be derived from it makes an attractive drilling target for the future.

The second notable indicator, potassium content, was first noticed at Site 909 where a bimodal distribution of K_2O was apparent. This increase from less than 3 wt% K_2O to more than 3 wt% occurs below the first occurrence of dropstones at this site, which suggests that it was a precursor indicator of the development of polar climate *via* the beginning (or strengthening) of sediment transport from nonlocal

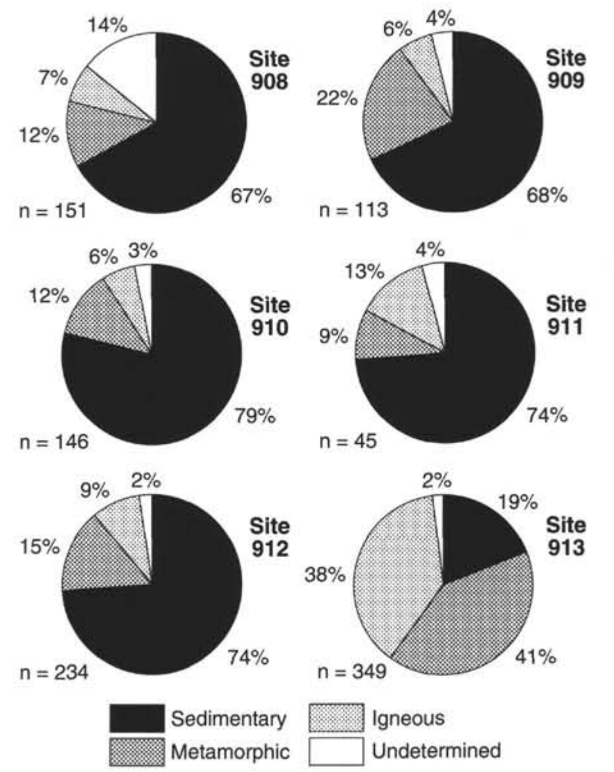

Figure 13. Relative abundances of various lithologic types of dropstones at Sites 908 through 913.

sources by ice rafting. With the clear clue from Site 909 it became obvious that the same change in K_2O content appeared in other holes from the Fram Strait-Yermak Plateau region. It remains to be seen in shore-based investigations whether these changes will be reflected in other indicators such as sediment mineralogy, trace element abundances, and isotope ratios.

Among the most interesting indicators in the interstitial waters were sulfate and silica. Sulfate generally dropped to zero within a few tens of meters of the sediment/water interface. At two sites, however, sulfate persisted in the column to the bottom of the deepest hole. The first of these sites, Site 907, shows evidence of circulation of fluids from below. In particular, the sulfate concentration actually rose with increasing depth in the upper half of the hole, then fell to about half of the seawater value at the bottom. At Site 913 sulfate shows the same peculiar behavior, persisting at substantial levels down to the bottom of Hole 913B. At both sites organic carbon is sufficiently abundant that sulfate should have been reduced in these sediments. Methane is very low at both sites. Certainly, methane and sulfate go to zero at the same depth in other cores from the region, methane decreasing upward and sulfate decreasing downward, with the two reaching zero at a redox boundary in the sediment. This leads to the suggestion that sulfate-reducing bacteria require (or perhaps just prefer) methane as an electron donor.

Dissolved silica in interstitial waters proved to be a potent predictor of the distribution of biosiliceous fossils at all sites on Leg 151. When silica was high (around 1000 mmol/L) siliceous fossils were present and usually well preserved. When silica levels fell to around 500 mmol/L, siliceous fossils were absent and, in at least one case from Site 913, the presence of lepispheres, indicative of the formation of opal CT was inferred by the sedimentologists. The most interesting phenomena displayed by dissolved silica were, however, the two instances of very low silica contents, around 100 mmol/L, indicating equilibrium with quartz. Both instances were in Paleogene sediments and were associated with sediments which were partially laminated.

Although both sodium and chloride contents of these interstitial waters were relatively high, suggesting a marine environment, the laminated sediments and lack of silica suggest an environment of restricted circulation that receives nutrient-depleted surface waters over a very shallow sill (well above the nutrient maxima usually around a depth of 1000 m in the modern ocean). Such a basin could become depleted in oxygen due to restricted circulation with terrestrial carbon supplying some of the oxygen-consuming potential. This is consonant with the occurrence of laminated sediments that, in turn, reinforces the suggestion of restricted deep water circulation and poor ventilation.

The chemical and isotopic work on samples from Leg 151 is just beginning and will continue into the future. Shipboard inorganic geochemistry has, however, proven to be an important and useful tool in the initial interpretation of drilling results.

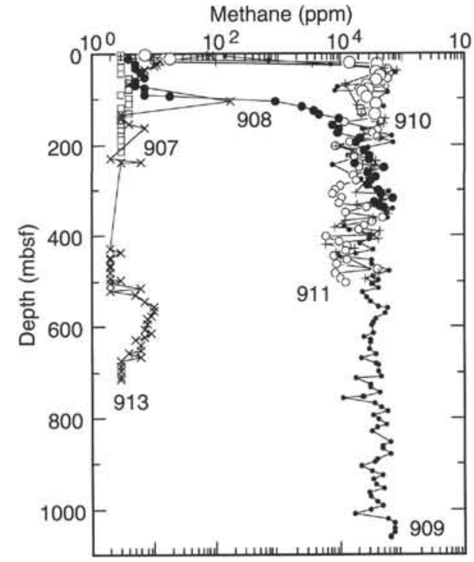

Figure 14. Methane abundance profiles of Sites 907–911 and 913.

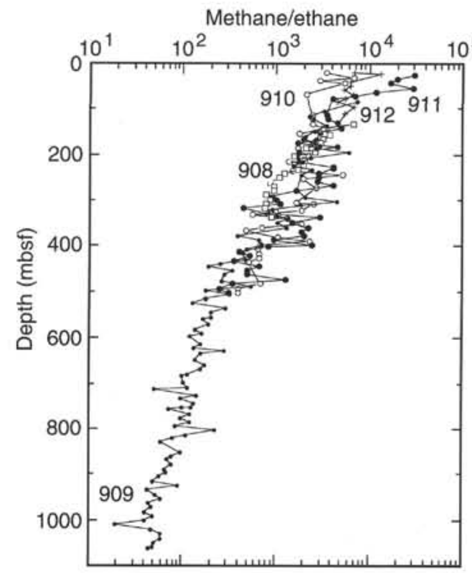

Figure 15. Depth profiles of methane/ethane ratio at Sites 908–912.

Organic Geochemistry

Hydrocarbon Gases: Safety Considerations, Depositional Environment, and Diagenesis

As part of the shipboard safety and pollution monitoring program, concentrations of methane (C_1), ethane (C_2), and propane (C_3) gases were routinely monitored for every core. Except for Sites 907 and 913, all Leg 151 sites are characterized by very high methane concentrations (Fig. 14). For safety considerations as well as for scientific reasons, it is important to know the origin of the hydrocarbons. Here, the C_1/C_2 ratio is used to get an initial idea about the origin of the hydrocarbons (i.e., to distinguish between biogenic gas and gas migrated from a deeper source of thermogenic hydrocarbons). Very high C_1/C_2 ratios indicate a gas (C_1) formation by microbiological processes. On the other hand, major amounts of C_2 (to C_5) are associated with thermogenic hydrocarbon generation. When interpreting the C_1/C_2 ratios, it has to be considered, however, that minor amounts of C_2 (and C_3, C_4, C_5) can also be generated in situ during early (low-temperature) diagenesis of organic matter. The importance of this process increases with increasing burial, resulting in a consistent ("normal") decrease in C_1/C_2 with increasing depth as recorded at numerous DSDP and ODP sites (JOIDES PPSP, 1992).

The C_1/C_2 ratios at Sites 908–912 are generally high, suggesting a biogenic origin of the methane. Furthermore, the records show the normal consistent decrease in C_1/C_2 ratios with increasing depth or temperature (Fig. 15). It is very probably formed by in-situ microbial fermentation of the marine organic carbon, which is present in major amounts in the lower part of the sedimentary sequence (see below). Similar in-situ microbial methane production from marine organic carbon resulting in high biogenic gas concentrations has also been described at other DSDP/ODP sites (e.g., at the Walvis Ridge; Meyers and Brassell, 1985). Furthermore, the rapid increase of methanogenesis begins immediately below the rapid depletion to zero of pore-water sulfate concentrations. These results support the microbial sulfate reduction-methane production model of Claypool and Kaplan (1974). At Sites 907 and 913, methane generation was inhibited by the presence of sulfate ions down to the bottom of the sites. Lower organic carbon values, a more terrigenous source of the organic matter and lower sedimentation rates recorded at Sites 907 and 913 may have caused these differences.

Although no obvious gas hydrates were observed at the Leg 151 sites, maximum concentrations of methane recorded in several shallow intervals may possibly be related to the presence of hydrates. According to the pressure-temperature stability field (cf. Kvenvolden and Barnard, 1983), geothermal temperature gradients between 60 and 90°C, water depths between about 600 and 3400 m, and bottom water temperatures of about 0°C, gas hydrates are stable down to about 100 to 300 mbsf at the different sites.

Hydrocarbon Formation at Site 909

At Site 909, higher molecular weight hydrocarbons also occurred in detectable amounts: isobutane, *n*-butane, isopentane, *n*-pentane, isohexane, *n*-hexane and *n*-heptane. The first downhole occurrence of these heavier hydrocarbons (such as hexane at about 700 mbsf or 60°C) and its consistent increase with increasing depth (or temperature) indicate the beginning of significant thermogenic hydrocarbon formation increasing farther downhole. Under these temperature conditions of >60°C, the occurrence of C_5–C_7 hydrocarbons and their smooth increase with depth is normal and has been reported in other DSDP and ODP sites (e.g., Sites 467 and 471; Whelan and Hunt, 1981; Site 603, Schaefer and Leythaeuser, 1987) where drilling was continued without incident. Thus, Site 909 drilling was also continued below 700 mbsf despite the occurrence of heavier hydrocarbons. At 1010 mbsf, however, a sharp major change in the hydrocarbons was recorded that, together with other geological observations, required the termination of drilling at 1061.8 mbsf. Rock-Eval data, which were not available at the time of the decision to continue or stop drilling, support the presence of distinctly increased amounts of free hydrocarbons (i.e., gas and/or oil) in the lowermost cores. This increase appears to be contemporaneous with an increase in total organic carbon contents suggesting increased in-situ hydrocarbon formation. The S2 values, a measure for the quantity of hydrocarbons that could be produced in these sediments by cracking the kerogen, are also higher in these lower cores. Detailed conclusions regarding thermal maturity and quality of the organic matter as well as further conclusions about migration and/or in-situ formation of hydrocarbons should be supported by other more precise geochemical methods, such as vitrinite reflectance and gas chromatography studies. According to the total organic carbon contents (1%–2.5%), S1 and S2 values of 0.4–0.9 mgHC/g rock and 2–6 mgHC/g rock, respectively, hydrogen index values of 150 to 250 mgHC/gC, and T_{max} values of up to 433°C, the sedimentary rocks recovered near the bottom of Hole 909C appear to be a source rock of good potential for gas and oil, with a still low level of thermal maturity (cf. Peters, 1986).

Organic Carbon and Paleoenvironments

In general, the total organic carbon (TOC) contents of the sediments recovered during Leg 151 are significantly higher than those typical for normal modern open-ocean environments (0.3%) They show, however, distinct variations in time and space (Fig. 16). The oldest sediments were drilled at Site 913 and are of earliest Oligocene to middle Eocene age. These sediments are characterized by high-amplitude variations in organic carbon contents between 0.2% and 5.5%. In the upper Oligocene sediments of Fram Strait, Sites 908 and 909, maximum TOC concentrations were recorded; most of them vary between 1% and 2%, with a maximum of 4.3%. The Miocene

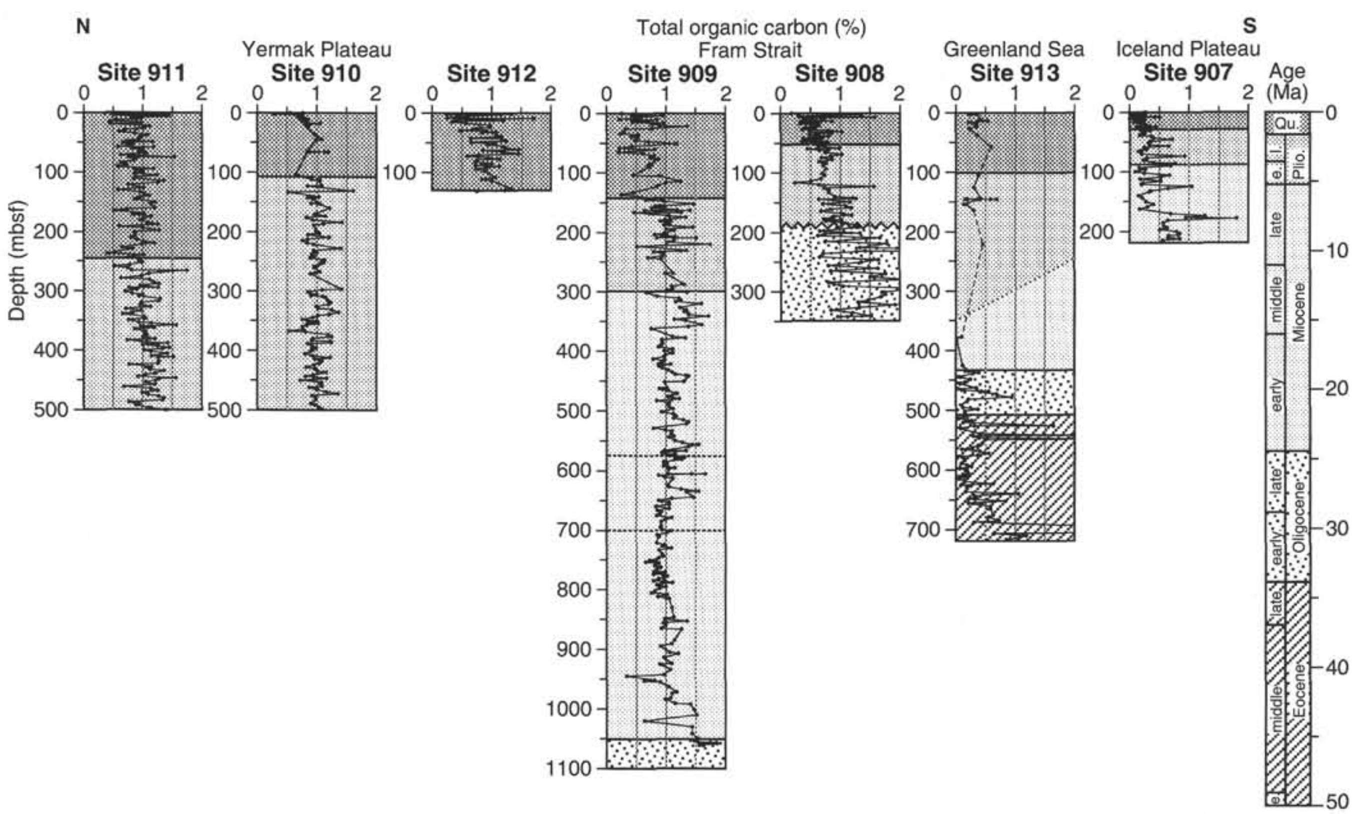

Figure 16. Summary of percent total organic carbon (TOC) in sediments recovered from Sites 907 through 913.

sediments recovered at Sites 907 and 909 display organic contents of 0.2% to 1.7%. In the Quaternary to Pliocene sediments, a general decrease in organic carbon content occurs from the Yermak Plateau Sites 910–912 (0.5%–1.7% TOC), to the Fram Strait Sites 908 and 909 (0.3%–1.5% TOC), to the Greenland Sea Site 913 (0.2%–0.6% TOC) and the Iceland Plateau Site 907 (0.1%–0.8% TOC).

To interpret the organic carbon data in terms of paleoenvironmental change it is absolutely necessary to have information about the composition of the organic matter (i.e., to distinguish between marine and terrigenous sources [e.g., Stein, 1991a, and further references therein]). The preliminary shipboard interpretation about the origin of the organic matter is mainly based on organic carbon/total nitrogen (C/N) ratios and, for a limited amount of samples, also on Rock Eval pyrolysis. The average C/N ratios of marine zoo- and phytoplankton are between 5 and 8, whereas higher land plants have ratios between 20 and 200 (Bordowskiy, 1965; Emerson and Hedges, 1988). When using C/N ratios as a source indicator, it has to be taken into account, however, that in organic-carbon-poor sediments the amount of inorganic nitrogen (fixed as ammonium ions in the interlayers of clay minerals) may become a major portion of the total nitrogen (Müller, 1977), causing (too) low C/N ratios. A second organic-carbon-type indicator, hydrogen index (HI) values derived from pyrolysis analysis, has been used (Éspitalié et al., 1977). In immature sediments, organic matter dominated by marine components has HI values of 200 to 400 mgHC/gC, whereas terrigenous organic matter has HI values of 100 mgHC/gC or less (e.g., Stein, 1991a). Also, the pyrolysis methods have their limits in organic-carbon-lean sediments (Katz, 1983; Peters, 1986). Thus, in intervals with TOC values <0.5% the C/N ratios as well as the pyrolysis data should be interpreted cautiously and supported by other methods (e.g., Stein, 1991a).

Based on the general dominance of C/N ratios <10, in all Leg 151 sites significant to dominant amounts of marine organic carbon were possibly preserved. The (limited) Rock-Eval data, on the other hand, suggest higher proportions of terrigenous material in large parts of the sedimentary sequences. Most of the peak values of organic carbon content of >1.5%, however, show distinctly higher C/N ratios as well, indicating the presence of major amounts of terrigenous material. A further strong argument for the presence of significant quantities of marine organic carbon at the Yermak Plateau and the Fram Strait sites is the occurrence of very high methane concentrations determined at these sites (see above).

Because changes in organic carbon concentrations can result from changes in both mineral components and organic carbon contents, the percentage values have to be transformed into mass accumulation (flux) rates before an interpretation of the data in terms of changes in organic carbon supply is possible (cf. van Andel et al., 1975). Based on shipboard stratigraphy and physical property data, flux rates were calculated for Quaternary and upper Pliocene intervals of the organic carbon rich sediments of Site 911 (Yermak Plateau) and the less-organic-carbon-rich sediments of Site 907 (Iceland Plateau). In general, the average mass accumulation rates of total organic carbon are low at Site 907, varying between 0.004 and 0.030 g cm^{-2} $k.y.^{-1}$. The minimum values occur in the upper Miocene to Quaternary intervals, with values similar to those observed in modern open-ocean oxic (low-productivity) environments (0.001 to 0.007 g cm^{-2} $k.y.^{-1}$; e.g., Stein, 1991a). In the middle Miocene, accumulation rates of organic carbon increase to about 0.020 to 0.030 g cm^{-2} $k.y.^{-1}$. At the Yermak Plateau Site 911, on the other hand, accumulation rates of organic carbon are distinctly higher throughout. In the late Pliocene to early Quaternary (3.5–1 Ma), they vary between 0.15 and 0.3 g cm^{-2} $k.y.^{-1}$. During the last 1 m.y., they decrease to values of 0.05 to 0.15 g cm^{-2} $k.y.^{-1}$.

Based on shipboard results, which suggest distinct long-term and short-term variations in marine and terrigenous organic carbon fluxes, the sedimentary records of Leg 151 sites provide an excellent opportunity for a detailed organic-geochemical study of the history of paleoceanic circulation patterns, surface-water productivity, and climatic change during late Cenozoic times. According to the shipboard results, the following important conclusions concerning organic carbon deposition and paleoenvironment can be made:

1. Very different processes must have controlled organic carbon deposition on the Yermak Plateau and in the Fram Strait area in comparison to the Greenland Sea and Iceland Plateau areas, as indicated by the distinct differences in flux and composition of the organic carbon fractions. The very high flux of marine and terrigenous organic carbon at the northern sites requires (paleo-) oceanographic conditions different from the normal open-ocean ones. Because the Yermak Plateau and Fram Strait sites are in the area strongly influenced by the relatively warm West Spitsbergen Current and the sea-ice cover, the interaction between both and their variations through time may be a dominant mechanism controlling the organic carbon deposition. Increased surface-water productivity near the ice edge might have caused increased marine organic carbon supply. Due to strong sea-ice melting, major amounts of terrigenous particles (i.e., organic as well as siliciclastic) are released from the ice and settle to the seafloor. This may explain the high flux rate of terrigenous organic carbon, but also the high flux rates of bulk sediment (which is mainly of terrigenous origin).
2. The flux of organic carbon decreased significantly from the late Pliocene to the Quaternary. The average accumulation rate of marine organic carbon on the Yermak Plateau prior to the major expansion of Northern Hemisphere glaciation at 2.6 Ma, was higher by a factor of 3–4 than the middle to late Quaternary rates. These drastic changes very probably reflect changes in sea-ice cover and West Spitsbergen Current intensity due to the extension of major Northern Hemisphere glaciation. A more increased sea-ice cover would certainly result in a decrease in surface-water productivity.
3. It appears to be possible to correlate long-term changes in organic carbon deposition during Miocene and Oligocene/Eocene times between records of Sites 907 and 909, and Site 913, respectively, to similar records at other ODP sites. The middle Miocene organic carbon maximum (as well as the middle Pliocene decrease) in organic carbon contents recorded at Sites 907 and 909 also occurs at Site 645 (Leg 105, Baffin Bay; Stein, 1991b). In the lowermost Oligocene/upper Eocene interval, the maximum contents of organic carbon at Site 913, which coincide with maximum occurrences of biogenic opal, can be correlated to the Labrador Sea (Site 647; Bohrmann and Stein, 1989). These intervals of increased organic carbon deposition, caused by increased terrigenous organic carbon flux and/or increased surface-water productivity, might reflect regional (or, if they correlate with similar records from other parts of the world oceans, global) paleoceanographic and/or paleoclimatic events.

Biostratigraphic Overview

Biostratigraphy in high northern latitudes is less well-constrained than time-equivalent counterparts in temperate and lower latitude seas, owing in part to the variable nature of carbonate and silica preservation in the Norwegian-Greenland Sea, low diversities and abundances of certain fossil groups, endemism, and faunas and floras that are less well-known and at least partially undescribed. Shipboard biostratigraphic studies on Leg 151 included analyses for calcareous nannofossils, planktonic and benthic foraminifers, diatoms, radiolarians, silicoflagellates, dinoflagellates, and *Bolboforma*. Each of these groups was represented in at least one of the sedimentary sequences recovered from the seven sites of Leg 151 (Fig. 17).

Quaternary and Pliocene sequences recovered from all of the far northern sites (Fram Strait, Yermak Plateau) and the East Greenland Margin contain microfossil assemblages composed predominantly of

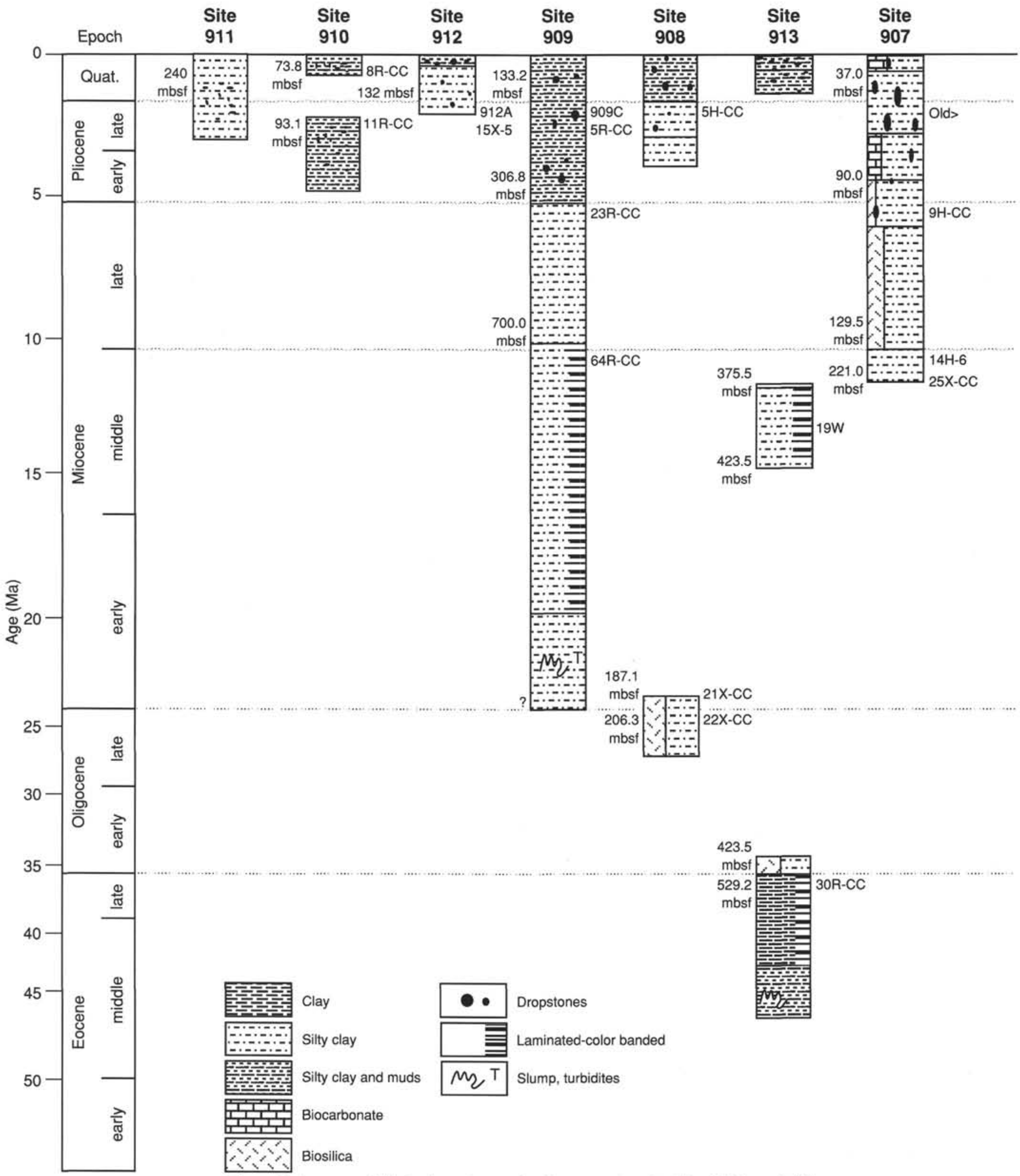

Figure 17. Summary of lithologies and ages of sediments recovered at Sites 907 through 913.

calcareous nannofossils, planktonic foraminifers, calcareous benthic foraminifers, and ostracods. Nannofossils and planktonic foraminifers are usually preserved in short sequences separated by barren intervals, although the planktonic foraminifer *Neogloboquadrina pachyderma* sin. Zone was found in a continuous sequence of 110- to 120-m thickness at Sites 909 and 911. The occurrences of calcareous benthic foraminifers are more continuous in all of the holes, and this group is present throughout the sequences at Sites 910, 911, and 912. Unfortunately, the degree of biostratigraphic resolution provided by benthic foraminifers is lower than that of the calcareous nannofossils and planktonic foraminifers. However, benthic foraminifers as well as ostracods provide valuable information on the conditions of bottom waters and the extent of ice rafting and reworking within the region (see "Cenozoic Environmental Evolution" section, this chapter). The greatest numbers of ice-rafted benthic foraminifers on this leg were recovered from the Yermak Plateau at Site 910 and in the lower part of Site 911. All three Yermak Plateau sites (910, 911, and 912) record an early Quaternary to late Pliocene calcium carbonate dissolution event. The cause of this dissolution is not known, but has also been observed in Leg 104 sediments on the Vøring Plateau.

Siliceous microfossils are absent from Quaternary and Pliocene glacial deposits with the exception of the uppermost Holocene sediments, rare diatom assemblages preserved in thin intervals at Site 908 (Pliocene *Thalassiosira kryophila* Zone) and Site 912 (lower Quaternary *Proboscia barboi*(?) Zone), and the well-preserved Pliocene biosiliceous sequence at Site 907 on the Iceland Plateau. The diatom assemblage at Site 908 is preserved in a narrow band (5 cm) associated with a highly siliceous volcanic ash layer, and probably should be interpreted as enhanced preservation of biogenic silica, rather than an episode of increased primary productivity in the Fram Strait during this interval. Rare, non-age-diagnostic dinoflagellates and radiolarian casts are present in Quaternary and/or Pliocene sediments at nearly all of the sites. Radiolarian tests tend to be strongly recrystallized and clay-filled, preventing any positive identifications at the species and genus levels. These rare occurrences of siliceous fossils in the far northern sites indicate that siliceous microorganisms were living in the water columns during these time periods, but conditions for preservation of biogenic opal were, and continue to be, unfavorable. Reworked siliceous microfossils, derived largely from Paleogene and Cretaceous source beds, occur in variable abundance in glacial sediments that lack an in-situ biosiliceous component.

The Miocene/Pliocene boundary was recovered at only two sites, Sites 907 and 909, and can only clearly be recognized at Site 907 on the basis of diatoms and radiolarians. The upper and upper middle Miocene were recovered at Site 907, and there is potential for at least two short hiatuses within the sequence. Diatom and radiolarian datums derived from biostratigraphic and magnetostratigraphic correlations elsewhere in the Norwegian-Greenland Sea (e.g., Goll and Bjørklund, 1989; Bodén, 1992) do not agree with biostratigraphic/magnetostratigraphic calibrations in the middle and upper Miocene (13–6 Ma) at Site 907. Calibrations at Site 907 suggest that radiolarian datums differ from those of the Vøring Plateau on the order of 2 to 4 m.y. At Site 913, middle Miocene siliceous microfossils were recovered in a wash core, which may have some relatively undisturbed sedimentary sequences, although the precise original depth of these sediments below seafloor is uncertain. A complete (or nearly complete) Miocene to uppermost Oligocene(?) section was recovered at Site 909 in the Fram Strait. This sequence contains only agglutinated foraminifers and sparse dinoflagellates, many of which are relatively long-ranging species. Based on dinoflagellate biostratigraphy, the boundary between the Pliocene and the Miocene at Site 909 is placed between 345 and 451 mbsf; the upper/middle Miocene boundary is tentatively at 576 mbsf. No other data, microfossil or magnetostratigraphic, are available from shipboard studies to refine these boundaries. Below 576 mbsf, the sequence contains rich and abundant assemblages of agglutinated benthic foraminifers. Although these assemblages are the same as those recorded from Oligocene and Eocene sequences of the North Sea, Labrador Sea, and the Vøring Plateau, co-occurring dinoflagellates at Site 909 support an age of late Oligocene to middle Miocene. Furthermore, calcareous nannofossils from a thin interval at the base of the hole also support an age of latest Oligocene to early Miocene. If these correlations are correct, this is the youngest recorded observation of these benthic foraminiferal assemblages, and indicates a very long-ranging diachrony of high-latitude agglutinated foraminifers.

Paleogene sediments drilled on Leg 151 include a 159.6-m-thick, lowermost Miocene/upper Oligocene sequence beneath an unconformity at Site 908 on the Hovgaard Ridge, and a lowermost Oligocene(?) to upper middle Eocene sequence at Site 913 on the East Greenland Margin. Both sequences are rich in biogenic silica (diatoms, radiolarians, and silicoflagellates); ebridians and *Bolboforma* are also present at Site 913. Agglutinated benthic foraminifers, dinoflagellates, and very rare calcareous microfossils confined to thin carbonate intervals occur within these siliceous sequences at both sites. The oldest sediments from Site 908 (Hovgaard Ridge, Fram Strait) are close in age to sediments at the bottom of Hole 909C (Fram Strait), which completely lacks biogenic silica, has sparse intervals of carbonate, and is dominated by an agglutinated benthic foraminifer assemblage with dinoflagellates. Post-cruise studies are necessary to determine if the biostratigraphic data support any stratigraphic overlap or if there is a hiatus between the two sequences. If these sequences are in fact co-eval, significant differences in lithologic and environmental characteristics between the two adjacent sites must be explained through tectonic and paleoceanographic reconstructions. Shore-based organic geochemical studies also need to focus on the relationship between the highly productive late Oligocene of Site 908 and the high concentration of heavy hydrocarbons near the base of Site 909, which forced a cessation of drilling at 1061.8 mbsf.

At Site 913, an excellent lower lower Oligocene/ upper Eocene biosiliceous interval is preserved at 462.0 mbsf. The fauna and flora in the upper part of this interval indicates an early early Oligocene to late Eocene age. Radiolarians dominate the fauna and flora in Core 151-913B-24R; diatoms strongly dominate the sediments below this interval in Cores -25R, -26R, and -27R. The biosiliceous interval is assigned to a previously unrecorded part of the Paleogene section of the North Atlantic and Norwegian-Greenland Sea, and appears to represent part of the stratigraphic gap between Oligocene sediments of Leg 105 and upper Eocene sediments of Leg 38. The Paleogene stratigraphic boundaries are poorly or very weakly defined in the high latitudes of the Northern Hemisphere, and the assemblages recovered at these sites will require extensive study to better define the ages of these sediments. Below the biosiliceous interval, only fragments of pyritized biosilica are preserved. The oldest sediments recovered during Leg 151, of middle Eocene age, are at the base of Hole 913B. This age is supported by middle Eocene dinocysts and *Bolboforma*, the latter being abundant enough to be called a "*Bolboforma* ooze."

Chronostratigraphy

A chronostratigraphic framework for the sedimentary sequences was established on the basis of integrated magnetostratigraphic and biostratigraphic results (Fig. 18). In general, the two methods yielded consistent chronologies, and in cases where one failed, the other method yielded a useful chronology. Paleomagnetic studies provided significant temporal constraints for most of the sedimentary sections that were sufficiently recovered and preserved during coring and drilling processes. With the exception of Sites 910 and 913, all of the sedimentary columns presented useful successions of magnetozones, which were correlated to the geomagnetic polarity time scale (GPTS) of Cande and Kent (1992). Further high-resolution chronostratigraphic control, especially within the Brunhes and Matuyama chronozones, is potentially available with the refined identification of short geomagnetic subchronozones such as the Emperor and Cobb Mountain subchronozones. Most of the Quaternary and upper Pliocene sedimentary sequences can be correlated between sites with enough precision to draw temporal correlation lines; the interpretation of the polarity record for the older sections is very preliminary.

There are few well-established biostratigraphic dates available for the high-latitude North Atlantic Ocean and Norwegian-Greenland Sea, partly due to sporadic sediment recovery of previous legs, difficulties in interpreting the previous magnetostratigraphy, and the endemic nature of many floras and faunas. Some of the most reliable datums available, which are used in the correlation of Leg 151 sites, are the Quaternary-Pliocene nannofossil events established in mid-

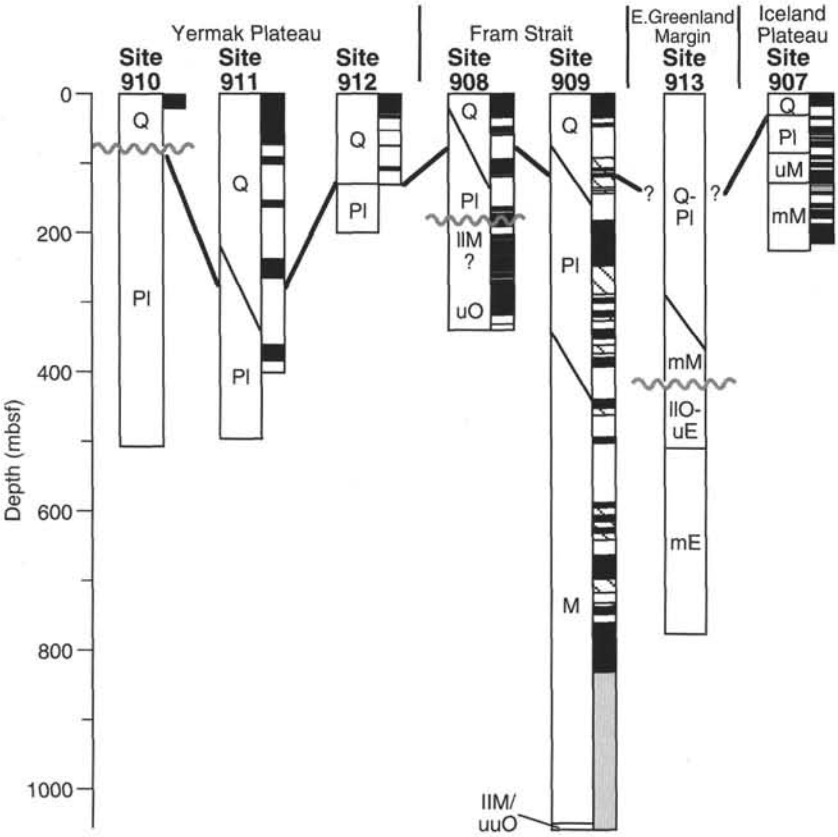

Figure 18. Stratigraphic correlation of the seven sites drilled during Leg 151, based on magnetostratigraphy and biostratigraphy. Correlation lines (heavy lines) between the sites are drawn for the Quaternary/Pliocene boundary. The unconformities are shown by wavy lines. Q = Quaternary; Pl = Pliocene; M = Miocene; uM = upper Miocene; mM = middle Miocene; llM = lower lower Miocene; uuO = upper upper Oligocene; uO = upper Oligocene; llO = lower lower Oligocene; uE = upper Eocene; mE = middle Eocene.

latitude North Atlantic Ocean (30°–50°N) (Sato et al., 1991). A number of diatom and radiolarian datums have been proposed by Bodén (1992) and Goll and Bjørklund (1989), respectively, from Leg 104 Vøring Plateau material based on correlation of first and last occurrence events of species with the magnetostratigraphy. However, in some intervals, particularly between 6.0 and 13.0 Ma, the microfossil datums are not well-dated. Calibration of detailed diatom and radiolarian biostratigraphy and magnetostratigraphy in Leg 151 sediments will provide an opportunity to confirm and/or revise the correlation of these datums to the geologic time scale.

Finally, although magnetozones are well-defined in most cores, some difficulties in the interpretation of the magnetostratigraphic record arose from several sources. Poor core recovery hindered the magnetostratigraphic interpretation of Sites 909, 910, 913, and to some extent Site 912; however, the most widespread impediment from these sites was the common occurrence of diagenetic iron monosulfides in the sediments. The magnetic remanence of large accumulations of iron monosulfide concretions dominates the NRM in some intervals of the sediment cores and hinders the interpretation of the magnetostratigraphy. Apparently, the very rapid sedimentation at these sites greatly exceeded the rate at which organic matter was oxidized in the sediments. After burial, this organic material produces reducing environments that favor the formation of the iron sulfides, but the mode of formation of these minerals and even their magnetic properties are poorly understood in many cases. Shipboard AF and thermal demagnetization experiments indicate that iron monosulfides may carry much of the NRM, even in intervals without visible significant concretions. Thus it is important to understand the diagenetic process whereby the iron monosulfides are formed and how reliably these minerals record geomagnetic field polarity. Another source of uncertainty in the interpretation of the magnetostratigraphy is the possibility of significant hiatuses in the sedimentation history. These hiatuses are also suggested by biostratigraphic studies, particularly in sedimentary sections at Sites 908 (Hovgaard Ridge), 910 (Yermak Plateau), and 913 (East Greenland Margin). Significant hiatuses are also likely at Site 909 (southern Fram Strait); however, incomplete recovery at this site prevented us from specifying their positions uniquely.

Sedimentation Rates

Sedimentation-rate curves of Holes 907A, 908A, 911A, and 912A for the last 5 m.y. and Hole 909A and 909C for the last 10 m.y. are plotted on Figure 19. Due to the limited number of biostratigraphic events, these curves are constrained mainly by the preliminary shipboard magnetostratigraphy. Sedimentation-rate curves for Sites 910

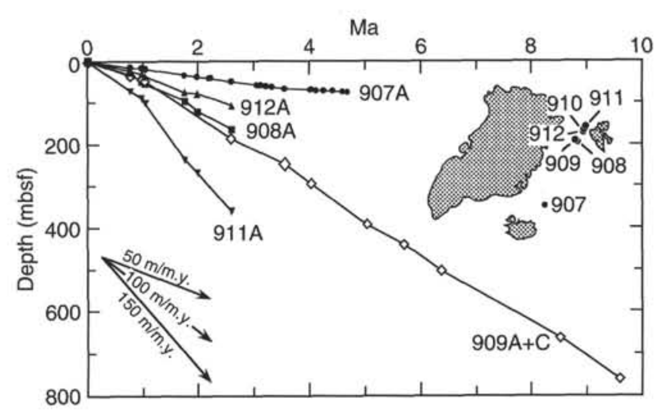

Figure 19. Sedimentation-rate curve for the Leg 151 sites, based mainly on magnetostratigraphy.

and 913 are not plotted owing to a poor magnetostratigraphic record and poor sediment recovery, respectively. The resulting curves show that the lowest sedimentation rates (~25 m/m.y.) during the last 5 m.y. are on the Iceland Plateau, Site 907. At all sites where reliable estimates were possible, the sedimentation rates generally accelerated in the Quaternary, often by as much as a factor of two. The intensification of the Northern Hemisphere glaciations, as observed by the frequency of dropstones during this interval, and the proximity of the Leg 151 sites to the surrounding ice sheets probably accounts for these high Quaternary sedimentation rates. However, a subsequent general relative decrease in the apparent sedimentation rate is observed from the beginning of the Jaramillo subchronozone at about 1 Ma. This decrease is defined by 2 or 3 calibration points including the lower and upper boundaries of the Jaramillo polarity chron, the Brunhes/Matuyama boundary, and perhaps the Emperor Event. These changes in the sedimentation rates may reflect major changes in the depositional environments of the North Atlantic-Arctic Gateways during the Quaternary, and further paleomagnetic studies will document more accurately their chronology.

Petrology of Crustal Rocks

Crystalline oceanic crust was drilled in only one hole, Hole 907A, where 4.9 m of tholeiitic basalt was recovered. The basalts are quenched with glassy rinds and very fine-grained chilled zones containing abundant vesicles and amygdules. Pillow structures are readily defined by glassy tops and bottoms with abundant vesicles on either side of the glassy areas. Neither sediments nor sedimentary rocks are intercalated with the pillow basalts. Basaltic magma was extruded into water as evidenced by pillow structures, and the presence of vesicles provides a rough estimate of water depth at extrusion: less than 500 mbsf.

The major and minor element chemistry of the pillow basalts reveals a relatively large range in composition, given that the pillows are juxtaposed and of small volume; however, Mg only ranges from 48 to 52 ($Mg = Mg^{2+}/(Mg^{2+} + Fe^{2+})$, Fe^{2+} calculated following Basaltic Volcanism Study Project (BVSP, 1981). Extremely low K_2O contents indicate that these tholeiitic basalts are most similar to N-MORB, rather than P-MORB. The basalts are only slightly altered as indicated by mineralogy; coherent compositional trends and relatively constant incompatible element ratios are supportive of this. Rock samples that are compositionally distinct (see Fig. 25 of "Site 907" chapter, this volume) could have suffered hydrothermal alteration, or they could be an indication of more than one magma source. Multiple magma sources are not unexpected due to the complex tectonic activity and history of this region.

CENOZOIC ENVIRONMENTAL EVOLUTION

Middle Eocene (Site 913)

The lowermost sediments at Site 913, the oldest material recovered during Leg 151, contain multiple fining-upward sediment gravity flows with coal and mud clasts, and laminations (Fig. 17). These sediments contain the highest abundances of terrigenous organic matter recovered during Leg 151. This suggests a site close to a continental source, possibly in an active tectonic or high sedimentation rate area, such as an early post-rift basin.

Above the mass-wasted sediment are finer-grained, interbedded, laminated and massive sediments, with moderate bioturbation. These sediments show a general fining-upward trend in the middle Eocene, suggesting a change in sediment source, depocenter, or possibly a tectonic barrier, preventing coarse sediment influx. The inorganic chemistry of the sediment shows little change, consisting of high silica continental sediments, derived from a granitic source. High terrigenous organic carbon values continue, although they also decrease through the middle Eocene. The abundance of fish teeth found in some samples from this interval suggests a low sedimentation rate.

Paleontological evidence from Site 913 suggests increasing productivity throughout the middle Eocene. Biogenic silica is preserved only in the upper middle Eocene. Decalcified *Bolboforma* and the absence of calcareous nannofossils, planktonic and benthic foraminifers suggest that this site was below the carbonate compensation depth (CCD). Similarities to agglutinated benthic foraminifers in the Labrador Sea indicate that there was at least partial connection with the North Atlantic.

Late Eocene to Early Early Oligocene (Site 913)

At Site 913 there is a renewed influx of terrigenous organic carbon (high C/N ratio) in the late Eocene, at approximately the same level as the first appearance of biogenic silica. The sediments themselves show little change, being interbedded, massive, and laminated silty clay and clay (Fig. 17). Upsection, however, they become very colorful, with exciting shades of blue, purple, and green. This coincides with an increase in the preservation and abundance of siliceous microfossils. Discrete siliceous ooze intervals were recovered and SiO_2 is also high in the pore waters. The siliceous intervals were probably formed during times of high productivity, resulting in high pelagic sedimentation rates and high organic carbon content. Based on the C/N ratio, these organic carbon values are interpreted to have a marine origin.

Upwelling probably caused the high productivity. Decay of organic matter results in low oxygen conditions in bottom waters and decreased bottom water pH, creating an environment corrosive to carbonate. As a result, calcareous microfossils are absent during this interval. Similarities to the agglutinated benthic foraminifers in the Labrador Sea suggest that the bottom waters were still in connection with the North Atlantic.

Late Oligocene to Early Early Miocene (Site 908, Site 909)

Evidence for this interval from Site 908 suggests moderately well mixed oceanic conditions in the Norwegian-Greenland Sea. The dominantly fine-grained and hemipelagic sediments record relatively high, but fluctuating surface water productivity. This is particularly well demonstrated by organic carbon values showing the highest variability of any Leg 151 site, generally between 0.75% and 1.5%, although some layers were over 2%. The average values are also higher than at most other Leg 151 sites. High productivity is further supported by the abundance of siliceous microfossils, with a diverse assemblage of diatoms and a low diversity assemblage of radiolarians. Absence of planktonic foraminifers, and the presence of rare nannofossils and benthic foraminifers place this site below the lysocline during this time. Intermediate bottom-water oxygen content is suggested by the benthic foraminiferal morphologies and the low diversity of the assemblage. Extensive bioturbation suggests at least intermediate levels of oxygen in the bottom waters, although thin, poorly bioturbated, laminated intervals suggest fluctuations to lower oxygen levels.

Middle Miocene (Site 913)

A glimpse of the middle Miocene is observed in the laminated clayey and sandy muds of Core 151-913B-19W, which contains a moderate abundance of siliceous microfossils with low diversity radiolarians and moderate diversity diatoms. Ebridians are also common. This suggests moderate, high pelagic productivity, although the organic carbon values are very low, <0.5%. Dissolution of all calcareous biota and the occurrence of a low diversity assemblage of siliceous agglutinated benthic foraminifers suggest that this site was below the CCD during this time.

Early to Late Miocene and Early Pliocene (Site 907, Site 909)

This interval is recovered in two dramatically different sections at Site 909 (Fram Strait) and Site 907 (Iceland Plateau) (Fig. 17). In the southern Norwegian-Greenland Sea, Site 907 indicates high productivity of siliceous microfossils, although preserved organic carbon is low, <0.5%. Terrigenous input is also low, and volcanic glass forms about 10% of the sediment. Diatoms suggest high productivity, perhaps related to upwelling conditions and an Atlantic source of surface water as in the modern ocean. The resulting lowered pH may have caused the dissolution of all carbonate. These oceanographic conditions were interrupted during two brief intervals with enhanced preservation of carbonate and deposition of the only nannofossil ooze recovered during Leg 151. Timing of these events is constrained by the calcareous nannofossils to late Pliocene Zones NN16– NN18 and late Miocene to early Pliocene Zones NN8–NN15.

At Site 909, in the Fram Strait, the lower Miocene to Pliocene interval suggests restricted oceanic circulation. On average, total organic carbon is slightly higher than 1%. The sediments show a general fining-upward trend. They alternate on a decimeter scale between massive, moderately to extensively bioturbated, and laminated, weakly to unbioturbated sediments, probably reflecting changing bottom water conditions and/or current strengths.

No biogenic silica or carbonate is preserved. Agglutinated benthic foraminifers indicate that very low oxygen bottom waters occurred during the late Miocene to early Pliocene, supporting the interpretation of corrosive bottom water conditions. The lowermost sediments at Site 909 contain a few, (possibly reworked?) Oligocene nannofossils.

The upper Oligocene?/lower Miocene section at Site 909 differs considerably from that at Site 908. This is a problem, as they are adjacent although at different depths (Site 908, 1273 mbsl; Site 909, 2519 mbsl). Perhaps there are undetected unconformities or environmental changes, or age differences not easily resolved by shipboard biostratigraphy, which can be invoked to explain these differences. The Miocene section at Site 913 is very different, but geographically far away. The laminations here, as with the laminated middle Eocene section at Site 913, may have been produced during intervals of reduced basin ventilation.

The oldest dropstone recovered during Leg 151 is from the latest Miocene at Site 907 (117 mbsf).

Pliocene to Quaternary (All Sites)

Pliocene and Quaternary sediments were recovered from all sites and are dominated by silty clay and muds. With the exception of Site 907, the first occurrence of dropstones at all sites, based on paleomagnetic ages, is in the lower Pliocene. At several sites (e.g., Sites 908, 909, 911) the onset of dropstones is preceded by an increase in potash (K_2O) concentration in the sediment, suggesting a change in the sediment source. Sediment composition appears to precede the onset of glacial dropstones. The increasing potassium trend continues as the abundance of dropstones increases, and then levels off at the higher value.

At about 2.5 Ma most sites show a substantial increase in dropstone abundance. Above this the variation in abundance and beginning of dropstone occurrence varies from site to site. In most sites, there is a substantial decrease in dropstone abundance in the upper Quaternary.

Microfossils are generally more common in this interval, especially in the younger part. Pre-glacial fossiliferous Pliocene sediments were recovered only at Site 910. The well-preserved, carbonate microfossil groups record good circulation and carbonate preservation at this shallow site. Organic carbon values average about 1%.

High glacial, especially Quaternary, sedimentation rates (>10 cm/k.y.) are recorded at the Yermak Plateau Sites 910, 911, and 912.

At least four sites (907, 909, 911, and 912) record a late Pliocene to Quaternary calcium carbonate dissolution event. This event was also observed on the Vøring Plateau. Dissolution of carbonate is caused by increased CO_2 in the bottom water.

The presence of biogenic sediments, particularly in the upper section (less than 50 mbsf) at most sites, suggests milder climatic conditions. These sediments are more colorful, with olive gray and very dark gray layers.

At Sites 908, 910, and 911, there is a steep downhole increase in the bulk density and strength over the top 20 to 30 mbsf (upper Quaternary), followed by a gradual decrease with depth. These are three of the four shallowest sites (1273, 556, and 901 mbsl, respectively). Data at the other shallow site, Site 912 (1037 mbsl) is not good enough to see any trend, although no obvious compositional changes were observed. The anomalously high values may be related to overcompaction due to ice, or may be a permafrost feature. This problem will be investigated in more detail when cores from the geotechnical hole, Hole 910D are studied.

FUTURE NORTHERN HIGH-LATITUDE DEEP-SEA DRILLING

After the successful North Atlantic legs of the Ocean Drilling Program (Legs 104, 105, 151, 152), the upcoming second NAAG leg, Leg 162 in 1995, and the North Pacific Transect leg, Leg 145 (Rea et al., 1993), which complemented earlier North Pacific DSDP Legs 18 and 19 (see "Introduction" chapter, this volume), the question remains if and how future deep-sea drilling can contribute to resolving the geological, environmental, and biological history of the Northern Hemisphere polar and subpolar deep-sea basins.

Once the second NAAG leg with its important scientific targets in the southern Norwegian-Greenland Sea and on both sides of the Greenland-Scotland Ridge is completed, many of the presently defined high priority drilling targets will have been exhausted. Many general and important paleoenvironmental problems, however, have only barely been touched upon and will, after careful assessment of the presently available data, probably require the Ocean Drilling Program to revisit the Northern Hemisphere polar and subpolar deep-sea basins. The problems include:

1. The Paleogene paleoceanography of the Norwegian-Greenland Sea;
2. The Paleogene history of Baffin Bay, tectonic evolution of the Baffin Bay mid-ocean ridge;
3. Nature and history of Labrador Sea bottom water renewal; nature of the thermohaline circulation prior to cold Northern Hemisphere climates;
4. Middle Miocene transition from preglacial to glacial paleoceanographies in the Norwegian-Greenland Sea, in particular in regions of Miocene ocean crust and along the East Greenland continental margin;
5. History of volcanic construction and tectonic subsidence of the entire Greenland-Scotland Ridge system with its sills and deep channels; history of hiatus formation and sedimentation to the immediate North and South of the ridge;
6. Overconsolidation of sediments along Arctic and subarctic continental margins;
7. Processes controlling formation and stability of Bottom Simulating Reflectors (BSRs) and of gas clathrates along Arctic and subarctic continental margins.

Considering only the available and established drilling techniques, the following future new high priority areas can be suggested to further study the Northern Hemisphere paleoenvironment:

1. Bering Sea: transition from a preglacial to a glacial paleoenvironment, variability of the glacial paleoceanography, origin of Bowers Bank, history of Bering Strait and of Beringia, water exchange with the Arctic Canada Basin.
2. Sea of Okhotsk: late Cenozoic paleoenvironments, areas of high fluid and gas exchange from the seafloor into the overlying water column (areas of highest methane export, seeps and their geological setting and history), Kamchatka and Kuril Island Arc volcanic and tectonic history, loess history, Sea of Okhotsk paleoceanography, and North Pacific deep and intermediate water renewal.
3. North Atlantic-Arctic: deep penetration on the shallow Yermak Plateau to establish nature and age of basement as well as of the overlying sediment column; establishment of a proper deep-water site close to the Yermak Plateau (deep marginal Arctic site); transect across one of the trough-mouth fans with the aim of correlation to the glacial history of the continental hinterland.

Considering alternative drilling platforms, the plans of the Nansen Arctic Drilling program (Thiede and NAD Scientific Committee, 1992) receive the highest priority. The program aims to bring deep-sea drilling into the permanently ice-covered Arctic Ocean to resolve its tectonic and paleoenvironmental history. Areas of high priority have been established:

1. Alpha-Mendeleev Ridge: sampling of the Mesozoic and lower Cenozoic preglacial pelagic sedimentary sequence of the Arctic Ocean; establishment of the age and nature of the volcanic basement.
2. Lomonosov Ridge: sampling of extended post-rift sedimentary sequence on top of the Lomonosov Ridge to establish timing of onset of the Arctic Ocean glaciation and of the variability of the depositional environments; sampling of syn- and pre-rift sediments.
3. Laptev Sea: intersection of the active mid-ocean Gakkel Ridge with the Laptev Sea continental margins; tectonic history of the area and nature of rifting. Paleoenvironment of high-resolution terrigenous sections in front of a large Arctic delta.
4. Chukchi Rise and Northwind Escarpment: tectonic history and opening of the Canada Basin and evolution of the Arctic Alaska passive margin.

Ms 151IR-113

Table 1. Site summary of Leg 151.

Hole	Latitude	Longitude	Water depth (mbsl)	Number of cores	Interval cored (m)	Core recovered (m)	Percent recovered (%)	Drilled (m)	Total penetration (m)	Time on hole (hr)	Time on site (days)
907A	69°14.989′N	12°41.894′W	1800.83	26	224.1	229.98	102.6	0.0	224.1	65.25	2.72
		Site 907 total		26	224.1	229.98	102.6	0.0	224.1	65.25	2.72
908A	78°23.112′N	01°21.637′E	1273.52	47	344.6	313.96	91.1	0.0	344.6	74.75	3.11
908B	78°23.125′N	01°21.644′E	1273.02	10	83.4	78.01	93.5	0.0	83.4	9.25	0.39
		Site 908 total		57	428.0	391.97	91.6	0.0	428.0	84.00	3.50
909A	78°35.065′N	03°04.378′E	2519.04	11	92.5	94.78	102.5	0.0	92.5	17.00	0.71
909B	78°35.074′N	03°04.380′E	2519.12	16	135.1	140.42	104.0	0.0	135.1	16.75	0.70
909C	78°35.096′N	03°04.222′E	2517.98	103	976.8	604.77	62.0	85.0	1061.8	268.50	11.19
		Site 909 total		130	1204.4	839.75	69.7	85.0	1289.4	302.25	12.59
910A	80°15.882′N	06°35.405′E	556.38	5	28.7	24.26	84.5	0.0	28.7	8.98	0.37
910B	80°15.876′N	06°35.451′E	556.98	2	15.4	15.37	99.8	0.0	15.4	3.75	0.16
910C	80°15.896′N	06°35.430′E	556.38	53	507.4	293.49	57.8	0.0	507.4	93.50	3.90
910D	80°15.881′N	06°35.424′E	556.54	18	160.6	103.46	64.4	0.0	160.6	28.25	1.18
		Site 910 total		78	712.1	436.58	61.3	0.0	712.1	134.48	5.60
911A	80°28.466′N	08°13.640′E	901.58	53	505.8	464.51	91.9	0.0	505.8	98.00	4.08
911B	80°28.476′N	08°13.636′E	900.98	15	112.1	112.89	100.7	0.0	112.1	7.00	0.29
911C	80°28.485′N	08°13.637′E	902.01	15	127.9	126.07	98.6	0.0	127.9	12.25	0.51
		Site 911 total		83	745.8	703.47	94.3	0.0	745.8	117.25	4.89
912A	79°57.557′N	05°27.360′E	1036.76	16	145.4	118.37	81.7	0.0	145.4	20.75	0.86
912B	79°57.533′N	05°27.397′E	1037.45	5	40.5	41.77	103.1	0.0	40.5	10.75	0.45
912C	79°57.523′N	05°27.363′E	1036.62	12	115.6	5.91	5.1	93.5	209.1	24.50	1.02
		Site 912 total		33	301.5	166.07	55.1	93.5	395.0	56.00	2.33
913A	75°29.344′N	06°56.830′W	3318.62	13	103.6	26.19	25.3	0.0	103.6	24.50	1.02
913B	75°29.356′N	06°56.810′W	3318.43	55	491.3	210.29	42.8	279.0	770.3	187.25	7.80
		Site 913 total		68	594.9	236.73	39.8	279.0	873.9	211.75	8.82
		Leg 151 total		475	4210.8	3004.55	71.4	457.5	4668.3	970.98	40.46